ornl

OAK RIDGE NATIONAL LABORATORY

LOCKHEED MARTIN

Assessment of the Available ^{233}U Cross-Section Evaluations in the Calculation of Critical Benchmark Experiments

L. C. Leal
R. Q. Wright

MASTER

Computational Physics and Engineering Division

ASSESSMENT OF THE AVAILABLE [233]U CROSS-SECTION EVALUATIONS IN THE CALCULATION OF CRITICAL BENCHMARK EXPERIMENTS

L. C. Leal
R. Q. Wright
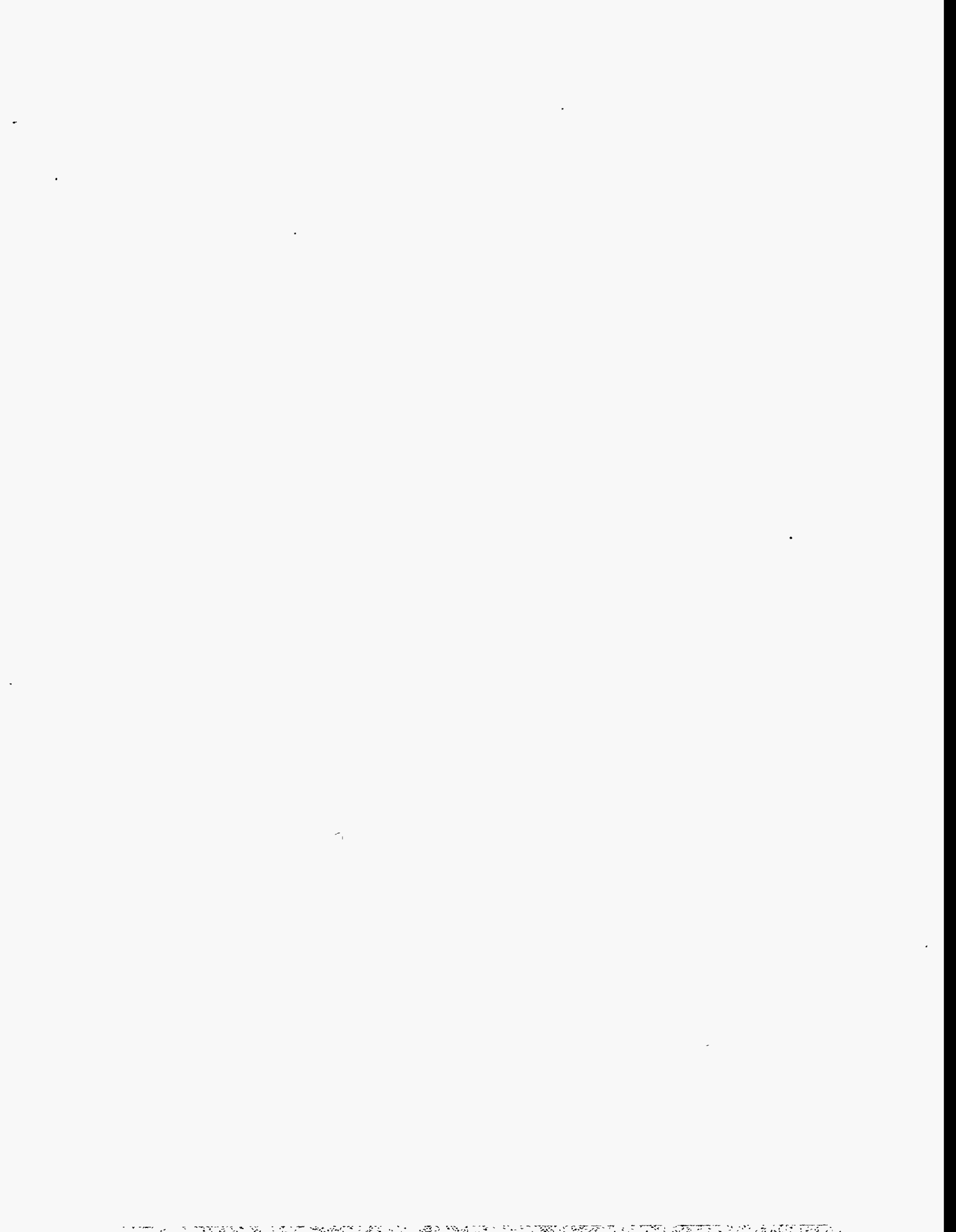
DISCLAIMER

Portions of this document may be illegible in electronic image products. Images are produced from the best available original document.

TABLE OF CONTENTS

LIST OF FIGURES

LIST OF TABLES

ACKNOWLEDGMENTS

The authors would like to thank C. W. Forsberg and K. R. Elam, Chemical Technology Division, for their support.
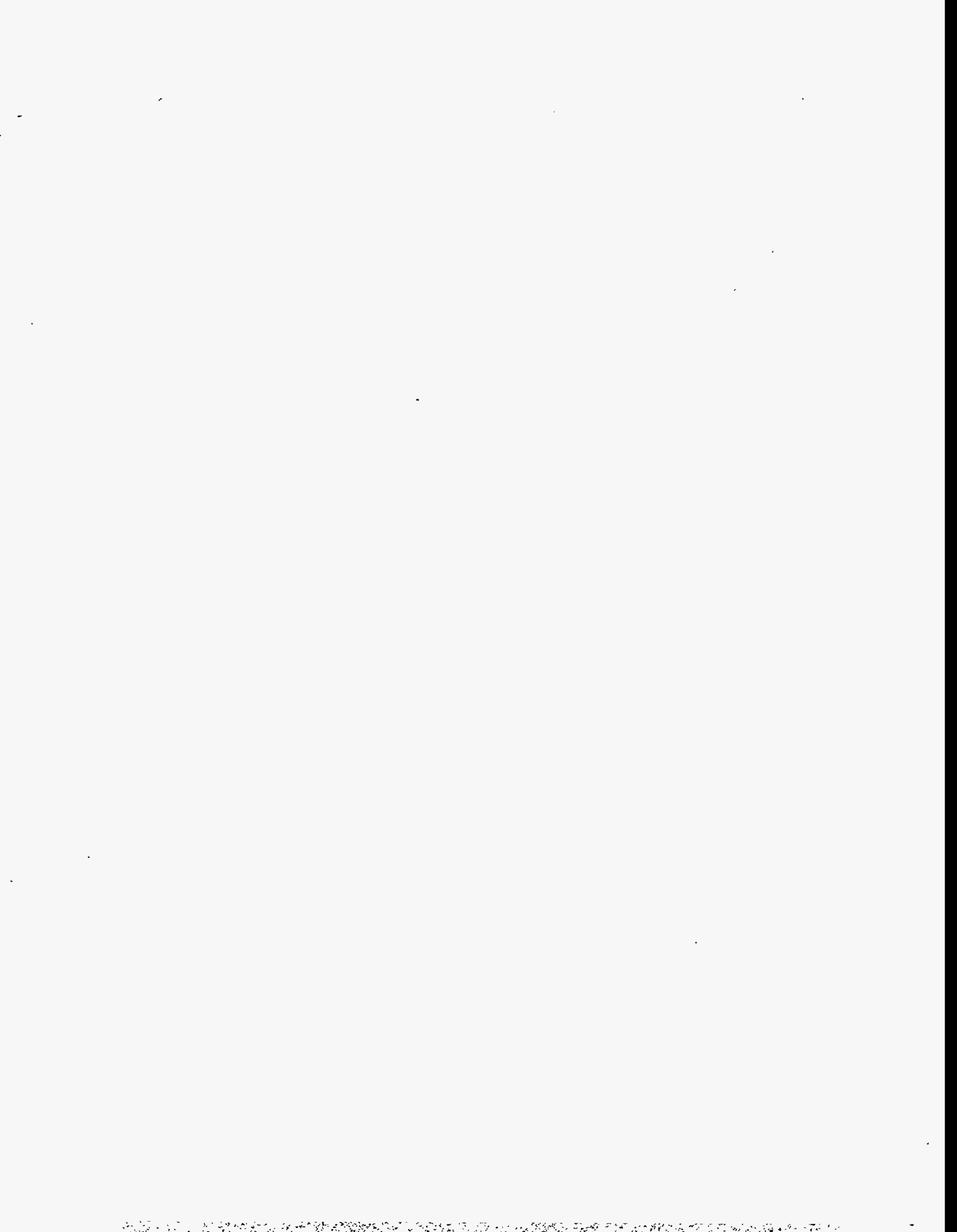
ABSTRACT

In this report we investigate the adequacy of the available ^{233}U cross-section data for calculation of experimental critical systems. The ^{233}U evaluations provided in two evaluated nuclear data libraries, the U. S. Data Bank [ENDF/B (Evaluated Nuclear Data Files)] and the Japanese Data Bank [JENDL (Japanese Evaluated Nuclear Data Library)] are examined. Calculations were performed for six thermal and ten fast experimental critical systems using the S_n transport XSDRNPM code. To verify the performance of the ^{233}U cross-section data for nuclear criticality safety application in which the neutron energy spectrum is predominantly in the epithermal energy range, calculations of four numerical benchmark systems with energy spectra in the intermediate energy range were done. These calculations serve only as an indication of the difference in calculated results that may be expected when the two ^{233}U cross-section evaluations are used for problems with neutron spectra in the intermediate energy range. Additionally, comparisons of experimental and calculated central fission rate ratios were also made.

The study has suggested that an ad hoc ^{233}U evaluation based on the JENDL library provides better overall results for both fast and thermal experimental critical systems.

1. INTRODUCTION

An assessment of the [233]U cross-section data available in the ENDF/B file [1] (Evaluated Nuclear Data File) and in the JENDL file[2] (Japanese Evaluated Nuclear Data Library) has been performed. The study consisted of examining in detail the performance of these data in the calculation of various critical systems. The selected critical systems are benchmarks with neutron energy spectra in the thermal and fast energy range. The lack of available benchmark data in the epithermal energy range preclude a complete estimate of the adequacy of the cross-section data for neutron spectra in the intermediate energy range. However, simple critical systems were made up to serve as an indication of the difference in calculated results that may be expected when these cross-section libraries are used.

In order to avoid any other source of bias, other than that due to the data, comparisons of the results are done for critical benchmark experiments corresponding to calculations carried out using similar calculational methodology. This includes the energy group structure and the theoretical method used. The selected energy group structures used in the calculations are the 238-group of the LAW library[3] and the 199-group of the VITAMIN-B6 cross-section library.[4] The calculations were done based on the discrete-ordinates one-dimensional (1-D) S_n transport theory included in the XSDRNPM code.[5]

A total of 16 benchmark calculations, 6 in the thermal and 10 in the fast energy range, were made. Additionally, four numerical benchmark cases with neutron energy spectra in the intermediate energy range were also done.

The 238-group library is based on data from ENDF/B-V, whereas the 199-group VITAMIN-B6 library contains ENDF/B-VI data. Calculations of the [233]U benchmarks were done for these two group structures. The [233]U cross-section data of the JENDL evaluation were processed, respectively, in the 238- and 199-group structure using the NJOY code system.[6] The [233]U evaluation included in the 238- and 199-group libraries was replaced by the JENDL evaluation with the following procedure: the SMILER module of the AMPX code system[7] was used to convert the NJOY library into the AMPX master library format. Consequently, the AJAX module was used to replace the existing [233]U data in the original 238- and 199-group libraries with the new processed [233]U data. A total of four cross-section libraries were used in the calculation of multiplication factors (k_{eff}) of the sixteen [233]U experimental benchmark systems and the four numerical benchmark cases with neutron energy spectra in the intermediate energy range. These four libraries consist of two for the 238-group structure, one with the [233]U ENDF/B evaluation and the other with the JENDL evaluation, and two for the 199-group structure.

2. GENERAL OVERVIEW OF THE AVAILABLE [233]U CROSS-SECTION DATA

The [233]U evaluations in ENDF/B Versions V and VI are identical. Both ENDF/B-V and ENDF/B-VI data for [233]U are based on a 1978 evaluation which employs the Adler-Adler formalism[8] to represent the resolved energy range cross sections. In these evaluations, the resolved energy range starts at 0.79 eV and extends up to 60 eV. Below 0.79 eV, the cross sections are given in the pointwise representation. In addition to that, a background cross-section file is given to correct for discrepancies between the experimental and calculated cross sections with the Adler-Adler representation. The main disadvantage of the background cross section is that it is not obtained based on a meaningful reaction theory, but is merely the values needed to make the resultant cross sections reproduce the experimental results.

The unresolved energy region in the ENDF/B-V (or VI) evaluation is from 60 eV up to 10 keV and is represented by average resonance parameters. Above 10 keV, up to 20 MeV, a pointwise representation of the cross sections is given.

The [233]U inelastic cross section, which impacts the calculation of fast benchmark systems, is a threshold reaction beginning at approximately 40 keV. Investigation of these data indicates that additional examination of the elastic and inelastic cross sections in the ENDF/B files is needed.

A more recent evaluation for [233]U in the resolved energy range was done a few years ago.[9] This analysis was performed with the reduced R-matrix Reich-Moore formalism[10] in the computer code, SAMMY.[11] The Reich-Moore formalism is appropriate for fissile isotopes like [233]U, since important features such as the level-level interference in the fission cross section are properly considered. Another important feature in this evaluation is that the resolved energy range was extended up to 150 eV to allow a better representation of cross-section energy self-shielding effects. This evaluation was adopted in JENDL. The unresolved energy range in the JENDL file is from 150 eV to 30 keV, and above 30 keV, a pointwise representation of the cross section is given. Likewise in ENDF/B, the adequacy of the elastic and inelastic cross sections of the [233]U in JENDL needs further investigation. Table 1 summarizes the overall status of ENDF/B-V and JENDL [233]U evaluations.

The [233]U total cross sections in the energy range from 1 to 30 eV computed with resonance parameters of ENDF/B and JENDL evaluations are compared with the experimental high resolution total cross-section data of Kolar.[12] The measured data were taken at a neutron flight path of about 100 m using the transmission method. Comparisons of the experimental total cross-section data (vertical bars) and the cross section calculated with the resonance parameters (solid line going into the data) are displayed in Fig. 1 for the ENDF/B evaluation, and in Fig. 2 for the JENDL evaluation, respectively. It is clear from Fig. 1 that above 3 eV the position of resonance energy in the ENDF/B evaluation is not properly defined; that is, the calculated cross section is shifted with respect to the experimental data. This feature is not present in the JENDL evaluation.

Table 1. Features of the ^{233}U ENDF/B and JENDL evaluations

	ENDF/B-V or VI	JENDL
Resolved energy range		
Energy range:	0.79 eV to 60 eV. Cross sections are represented as pointwise below 0.79 eV	10^{-5} to 150 eV. No pointwise representation of the cross sections at low energies
Formalism:	Adler-Adler (converted from a Reich-Moore evaluation performed in the late 1960s)	Reich-Moore (rigorous representation of the cross sections)
Background cross section:	Yes (not suitable for temperature effects)	No (no problem for temperature effects)
Cross-section representation:	Good	Very good
Unresolved energy range		
Energy range:	60 eV to 10 keV. Pointwise cross-section representation from 10 keV to 20 MeV	150 eV to 30 keV. Pointwise cross-section representation from 30 keV to 20 MeV
Formalism:	Average resonance parameters given. Sampling according to defined resonance parameter distribution	Average resonance parameters given. Sampling according to defined resonance parameter distribution
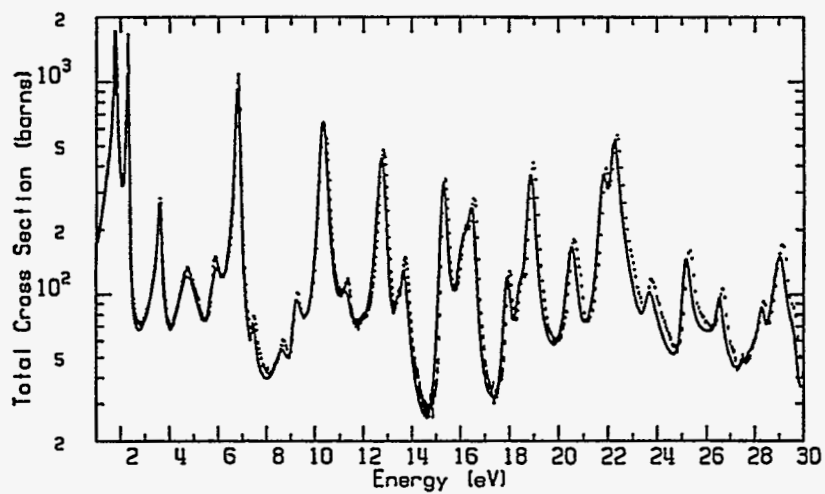
Fig. 1. Comparison of experimental (vertical line) and calculated (solid line) [233]U total cross sections for the ENDF/B evaluation.
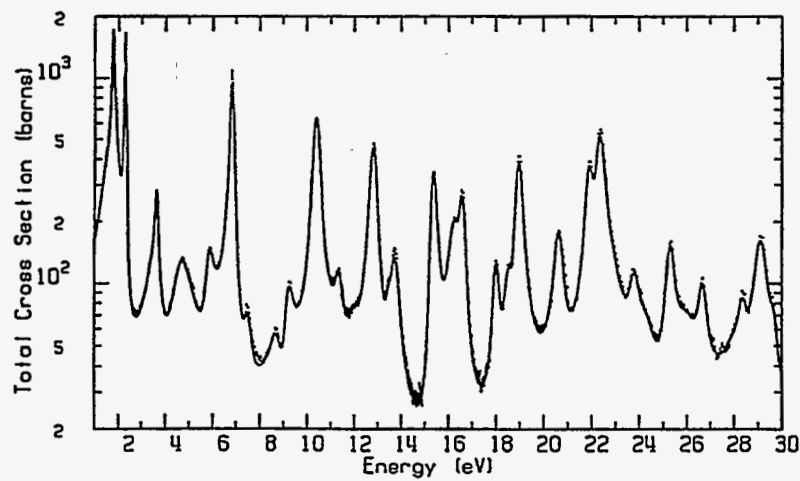
Fig. 2. Comparison of experimental (vertical line) and calculated (solid line) [233]U total cross sections for the JENDL evaluation.

4

3. COMPARISON OF THE ENDF/B AND JENDL EVALUATIONS

Calculations of benchmark systems were performed with both ENDF/B and JENDL data for the 238- and 199-group structures. Point cross-section data were generated with the NJOY code system using a reconstruction tolerance of 0.001, respectively, in the RECONR module (reconstruction of the temperature-independent cross section from resonance parameters) and BROADR (calculation of the Doppler broadening effects on the cross section). The NJOY procedures to generate the 238- and 199-group cross-section libraries are given in Appendix A. Thermal parameters at 0.0253 eV calculated with NJOY with the 199-group structure are shown in Table 2. The first column displays the experimental values, whereas columns two and three are results based on the ENDF/B and JENDL evaluations, respectively. Also included in Table 2 are the resonance integrals, fission and capture, and the ratio capture-to-fission, that is, the α-value defined as

$$\alpha = \frac{\displaystyle\int_{0.5\,eV}^{20MeV} \frac{\sigma_\gamma(E)}{E} dE}{\displaystyle\int_{0.5\,eV}^{20MeV} \frac{\sigma_f(E)}{E} dE} \quad , \tag{1}$$

where σ_γ is the gamma capture cross section and σ_f is the fission cross section.

The numerator and denominator of Eq. (1) are, respectively, the definitions of the $1/E$ weighted capture resonance integral and fission resonance integral, which are also given in Table 2.

Table 3 displays the fast cross-section data averaged over the fission spectrum for the two ^{233}U evaluations. These values were extracted from the NJOY PENDF files using the program INTER which is maintained at the National Nuclear Data Center (NNDC).[13] Tables 2 and 3 indicate substantial differences in the cross-section values of ENDF/B and JENDL evaluation mainly in the fast energy range. In the thermal energy range, the elastic cross section differs by as much as 5%. The differences in the ^{233}U cross sections in the two evaluations in the fast energy range appear in the inelastic cross section ($\sim$33%) and in the capture cross section (37%).

5

Table 2.Comparison of the thermal cross sections (0.0253 eV) of the ^{233}U
ENDF/B and JENDL evaluations

Values at 0.0253 eV	Experimental (barns)	ENDF/B-V (barns)	JENDL (barns)	Percentage difference between JENDL and ENDF/B
Total cross section	587.4	587.79	589.40	0.27
Elastic cross section	12.8±0.3	12.64	11.99	-4.99
Fission cross section	529.1±1.2	528.89	531.42	0.48
Capture cross section	45.5±0.7	45.81	45.28	-1.16
ν	2.493±0.004	2.4947	2.4930	-0.07
η	2.296±0.004	2.2958	2.2973	0.07
g_f	0.9955±0.0015	0.9974	0.9977	0.03
g_c	–	1.0273	1.0324	0.50
Resonance integral: fission	760±17	756.94	774.50	2.32
Resonance integral: capture	137±6	136.67	138.51	1.35
α	–	0.1806	0.1788	-1.00

Table 3. Comparison of the fast cross sections of the ^{233}U ENDF/B and JENDL evaluations

Fast cross sections (fission spectrum averaged)	ENDF/B (barns)	JENDL (barns)	Percentage difference
Total	7.4953	7.5148	0.26
Elastic	4.6154	4.2636	-7.62
Inelastic	0.9363	1.2481	33.3
Fission	1.8928	1.9360	2.28
Capture	0.0470	0.0644	37.0
ν (at 1 MeV)	2.57228	2.5720	-0.01

4. COMPARISONS OF CRITICAL BENCHMARK CALCULATIONS USING ^{233}U ENDF/B AND JENDL EVALUATIONS

Benchmark calculations of the sixteen ^{233}U critical experiments, six thermal and ten fast, and four numerical benchmark systems with energy spectra in the epithermal energy range, were performed with the four libraries. The characteristics of these critical benchmark experiments are given in Table 4. The calculated multiplication factors (k_{eff}) were obtained with the 1-D S_n transport code, XSDRNPM. All of the XSDRNPM calculations were done with the CSASN sequence, BONAMI, NITAWL, and XSDRNPM, of the SCALE-4.3 system.[14]

The six ORNL critical thermal benchmark experiments are homogeneous unreflected spheres of ^{233}U and light water.[15] These benchmark systems are useful to test the adequacy of the cross sections of the fissile material, ^{233}U, in the thermal energy range. The XSDRNPM calculations were carried out with an S_8 angular quadrature and a P_3 scattering order. The CSASN input descriptions of the six ORNL critical benchmark experiments are given in Appendix B. Table 5 shows the k_{eff} results for XSDRNPM calculations performed with the 199-group VITAMIN-B6 cross-section data library, which is based on the ENDF/B-VI evaluation. Column 1 lists the k_{eff} values calculated with ^{233}U cross-section data ENDF/B, and column 2 gives the results using JENDL data. A close look at Table 5 reveals that the k_{eff} results of calculations with the ^{233}U evaluation in the JENDL file are much better than those obtained using the ^{233}U evaluation in the ENDF/B library. In fact, the average k_{eff} obtained with the JENDL ^{233}U evaluation is excellent. This indicates that the parametric representation of the ^{233}U cross sections in the resolved energy range is better than that in the ENDF/B library. Similarly, k_{eff} calculations have also been performed for the 238-group library. The results are displayed in Table 6. These results also indicate that the ^{233}U JENDL evaluation is better than ENDF/B for thermal benchmark experiments. Note that all differences quoted in these results are related to the ^{233}U cross section.

Calculations of k_{eff} for ten ^{233}U fast benchmark experiments[15] using XSDRNPM with the 238- and 199-group structures were also done. The CSASN input descriptions of these critical benchmark experiments are given in Appendix C. These benchmarks correspond to unmoderated spheres containing ^{233}U, which may be a bare sphere, a sphere reflected with an intermediate mass element, or a sphere surrounded by natural uranium or its isotopes, ^{235}U and/or ^{238}U. In the XSDRNPM calculations of these benchmarks an S_{32} angular quadrature and a P_3 scattering order appeared to be sufficient to reproduce the experimental results. Table 7 compares the calculated k_{eff} values for these ^{233}U fast benchmarks using the 199-group VITAMIN-B6 library for ^{233}U for the ENDF/B and JENDL evaluations. In contrast to the thermal range, the JENDL results indicate that the fast cross sections in the JENDL library do not reproduce k_{eff} well. In fact, the calculated k_{eff} values using the ^{233}U JENDL evaluation are higher than the experiments by as much as 2%, and the average of the ten benchmarks is ~1.1% higher. The overall results of the calculated k_{eff} with the ^{233}U ENDF/B evaluation appears to be better than the JENDL in the fast region. A noticeable difference between the two ^{233}U evaluations in the fast energy range is that the energy dependence of the inelastic cross sections of the two libraries differs substantially. At this point, no attempt has been made to verify the cause of the discrepancy. The inelastic cross section impacts the leakage, which, in turn, affects the k_{eff}. Figure 3 shows the ^{233}U inelastic cross sections for the ENDF/B and JENDL evaluations. It is also noted that the

Table 4. Features of the ^{233}U critical benchmark experiments

Benchmark	H/U atom ratio	wt % ^{233}U	U density (g/cm^3)	Geometry	Reflector
Thermal					
ORNL-5	1533	97.70	-	sphere	none
ORNL-6	1470	97.70	-	sphere	none
ORNL-7	1417	97.70	-	sphere	none
ORNL-8	1369	97.70	-	sphere	none
ORNL-9	1324	97.70	-	sphere	none
ORNL-11	1986	97.70	-	sphere	none
Fast					
^{233}U-MET-FAST-001 (JEZEBEL-23)	-	98.2	18.424	sphere	none
^{233}U-MET-FAST-002-a	-	98.2	18.621	sphere	HEU
^{233}U-MET-FAST-002-b	-	98.2	18.644	sphere	HEU
^{233}U-MET-FAST-003-a	-	98.2	18.621	sphere	NU
^{233}U-MET-FAST-003-b	-	98.2	18.644	sphere	NU
^{233}U-MET-FAST-004-a	-	98.2	18.621	sphere	W
^{233}U-MET-FAST-004-b	-	98.2	18.644	sphere	W
^{233}U-MET-FAST-005-a	-	98.2	18.621	sphere	Be
^{233}U-MET-FAST-005-b	-	98.2	18.644	sphere	Be
FLATTOP-23	-	98.2	18.419	sphere	NU

Table 5. Comparison of ENDF/B and JENDL ^{233}U evaluations for ORNL
thermal benchmarks for the 199-group library

Benchmark	ENDF/B	JENDL
ORNL-5	0.9968	0.9997
ORNL-6	0.9972	1.0002
ORNL-7	0.9970	0.9999
ORNL-8	0.9969	0.9999
ORNL-9	0.9963	0.9993
ORNL-11	0.9954	0.9980
Average	0.9966	0.9995

Table 6. Comparison of ENDF/B and JENDL ^{233}U evaluations for ORNL
thermal benchmarks for the 238-group library

Benchmark	ENDF/B	JENDL
ORNL-5	0.9963	1.0010
ORNL-6	0.9967	1.0014
ORNL-7	0.9965	1.0011
ORNL-8	0.9963	1.0011
ORNL-9	0.9957	1.0004
ORNL-11	0.9957	0.9998
Average	0.9962	1.0008

Table 7. Comparison of ENDF/B and JENDL ^{233}U evaluations for ORNL
fast benchmarks for the 199-group library

Benchmark	ENDF/B	JENDL
^{233}U-MET-FAST-001 (JEZEBEL-23)	0.9929	1.0125
^{233}U-MET-FAST-002-a	0.9952	1.0093
^{233}U-MET-FAST-002-b	0.9975	1.0088
^{233}U-MET-FAST-003-a	0.9958	1.0100
^{233}U-MET-FAST-003-b	0.9971	1.0085
^{233}U-MET-FAST-004-a	1.0027	1.0172
^{233}U-MET-FAST-004-b	1.0061	1.0181
^{233}U-MET-FAST-005-a	0.9949	1.0094
^{233}U-MET-FAST-005-b	0.9974	1.0097
FLATTOP-23	1.0004	1.0088
Average	0.9980	1.0112

U-233 Inelastic Cross Section
ENDF/B-VI vs. JENDL-3
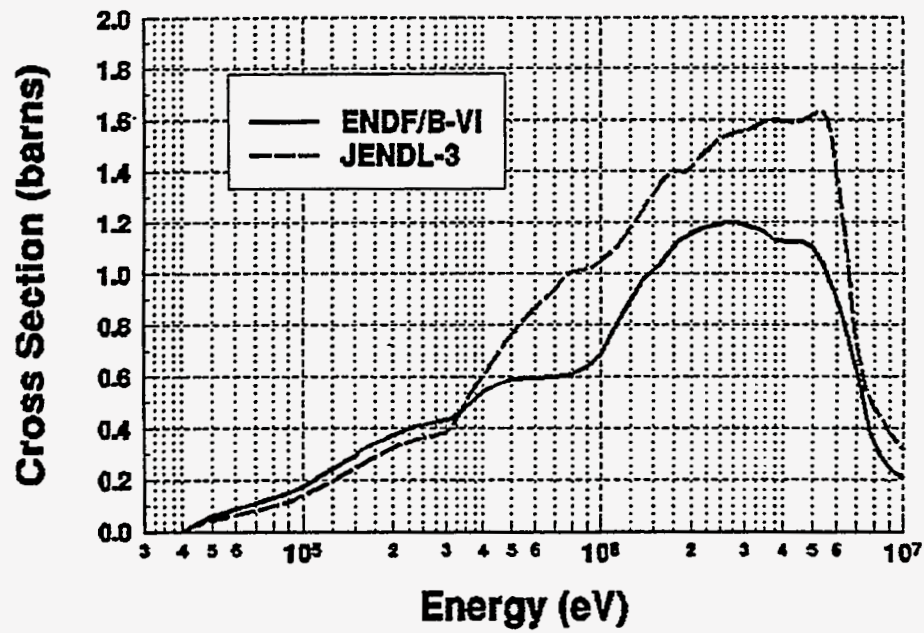
Fig. 3. Comparison of the ENDF/B-VI and JENDL-3 inelastic cross sections.

11

[233]U fast fission cross sections of the two evaluations are about the same up to 1 MeV. Above 1 MeV, the JENDL evaluation has a larger fission cross section value than that of the ENDF/B. The calculations with the 238-group library are shown in Table 8.

Table 8. Comparison of ENDF/B and JENDL [233]U evaluations for ORNL
fast benchmarks for the 238-group library

Benchmark	ENDF/B	JENDL
[233]U-MET-FAST-001 (JEZEBEL-23)	0.9934	1.0126
[233]U-MET-FAST-002-a	0.9959	1.0098
[233]U-MET-FAST-002-b	0.9982	1.0093
[233]U-MET-FAST-003-a	0.9973	1.0110
[233]U-MET-FAST-003-b	0.9990	1.0099
[233]U-MET-FAST-004-a	1.0034	1.0177
[233]U-MET-FAST-004-b	1.0058	1.0176
[233]U-MET-FAST-005-a	0.9983	1.0124
[233]U-MET-FAST-005-b	1.0014	1.0135
FLATTOP-23	1.0011	1.0091
Average	0.9994	1.0123

In addition to the benchmark calculations presented previously, comparisons of experimental central fission rate ratios with calculations performed using the ENDF/B and JENDL [233]U evaluations have also been carried out. The experimental data consist of measurements of the fission reaction rates of an isotope and measurements of the fission reaction rate of an isotope utilized as the standard.[15] Foils containing the isotope for which reaction rates are to be measured are inserted in the center of a critical system, and consequently the fission reaction rates (i.e., $\int \sigma_f(E) \phi(E) dE$) are measured. The Cross Section Evaluation Working Group (CSEWG) has adopted [235]U as a standard.[16] For an isotope x, the central fission ratio (cfr) is

$$cfr = \frac{\int \sigma_f^x(E) \, \phi(E) \, dE}{\int \sigma_f^{235U}(E) \, \phi(E) \, dE} \, , \tag{2}$$

12

where σ_f^x is the fission cross section of isotope x and $\sigma_f^{235_U}$ is the ^{235}U fission cross section. Table 9 illustrates the comparisons of experimental ^{233}U fission reaction rate ratios measured in four fast systems, namely JEZEBEL, GODIVA, FLATTOP-25, and BIGTEN. The result displayed in column 2 is the experimental data,[15] whereas columns 3 and 4 show the calculated-to-experimental ratio (C/E) for ENDF/B and JENDL for the 199-group structure. The ENDF/B calculated ^{233}U/^{235}U fission-rate ratios appear to be in better agreement with the measured values than the JENDL results. The explanation for the higher JENDL ^{233}U/^{235}U fission ratios in Table 9 and the higher values for the JENDL k_{eff} values in Tables 7 and 8 appear to be that the JENDL fission cross section is about 2% higher than ENDF/B for the energy range 0.9 to 6 MeV.

Table 9. Comparison of ENDF/B and JENDL ^{233}U/^{235}U fission central
reaction rate ratios with measured values

Benchmark	Experiment	ENDF/B (C/E)	JENDL (C/E)
JEZEBEL	1.578±1.7%	1.000	1.016
GODIVA	1.590±1.9%	1.001	1.012
FLATTOP-25	1.595±1.9%	0.990	1.007
BIGTEN	1.580±1.9%	0.996	0.992

5. RESULTS OF CALCULATIONS OF ^{233}U NUMERICAL BENCHMARK SYSTEMS

The lack of ^{233}U critical benchmark experiments with energy spectra peaking in the intermediate energy range is a serious limitation which prevents complete testing of the available ^{233}U cross sections for critical systems in this energy regime. There is an urgent need to identify reliable benchmarks or perform new experiments for systems with spectra peaking in the intermediate energy range, as this relates closely to real situations involving ^{233}U.

In the absence of real benchmarks, four fictitious critical benchmark problems with energy spectra where the fission-rate-per-unit-lethargy peaks in the epithermal region have been constructed. These fictitious benchmarks will be used in calculations using ^{233}U from both the ENDF/B-VI and JENDL-3 evaluations. It is not possible to determine which evaluation is better; however, we can determine how much the calculated k_{eff} values differ. This information will be useful in accessing the impact ^{233}U has on intermediate range situations.

In the determination of the benchmark parameters, the nuclide concentrations and dimensions were adjusted until the calculated k_{eff} using the ENDF/B-VI ^{233}U evaluation was approximately equal to 1.0 (third column of Table 10). The SCALE input for the four fictitious benchmarks is given in Appendix D. The first two benchmarks, Cases A and B, are mixtures of uranyl-fluoride and heavy water in spherical configurations with a stainless steel vessel reflected by heavy water. The nuclide concentrations and the diameters of the spheres varies, but both cases are reflected by 10.7 in. of D_2O. Case C is an infinite homogeneous medium of uranium (about 82 wt % ^{233}U) and graphite, also containing a significant quantity of boron. The graphite-to-^{233}U ratio is 772 and the ^{10}B-to-^{233}U ratio is 0.586. The effect of the high ^{10}B concentration in this benchmark drastically reduces the fluxes and fission rates below 1 eV. Case D is an 18-in.-diam mixture of uranyl-fluoride and heavy water in a sphere with an aluminum vessel and no reflector.

Calculations were performed with XSDRNPM using the 199-group ENDF/B-VI cross-section library. The calculated k_{eff} values are shown in Table 10. The energy corresponding to the average lethargy of fission (AEF) from this calculation is also given in the second column of Table 10. The k_{eff} calculations using the JENDL ^{233}U evaluation are shown in the fourth column of Table 10. The calculated fission-rate-per-unit-lethargy using the ENDF/B-VI ^{233}U evaluation is shown in Figs. 4–7.

In comparing the ENDF/B-VI and JENDL-3 calculations in Table 10, we observe that the cases A, B, and D agree fairly well. These cases are the uranyl-fluoride heavy-water solutions. The AEF (see Table 10) and the calculated fission rates (see Figs. 4 and 7) for cases A and D are quite different. The good agreement in the calculated k_{eff} values using the ENDF/B-VI and JENDL-3 ^{233}U evaluations is probably due to compensating differences in the calculated fission and absorption rates in different energy ranges.

For case C (infinite homogeneous uranium graphite) the calculated k_{eff} using ENDF/B-VI and JENDL-3 differs by 1.35%. This is a large difference compared to that seen for cases A, B, and D. About all that can be said is that this case has a much different composition, has no leakage, and that the spectrum is different. Apparently any compensating differences in the fission and absorption rate are less effective than for the other benchmarks.

Table 10. Calculations of the k_{eff} for four numerical
benchmark cases with 199-group structure

Case	AEF(eV)	ENDF/B	JENDL
A	2.72	1.0006	1.0022
B	16.7	1.0015	1.0025
C	33.1	1.0000	1.0135
D	628.0	1.0002	1.0019
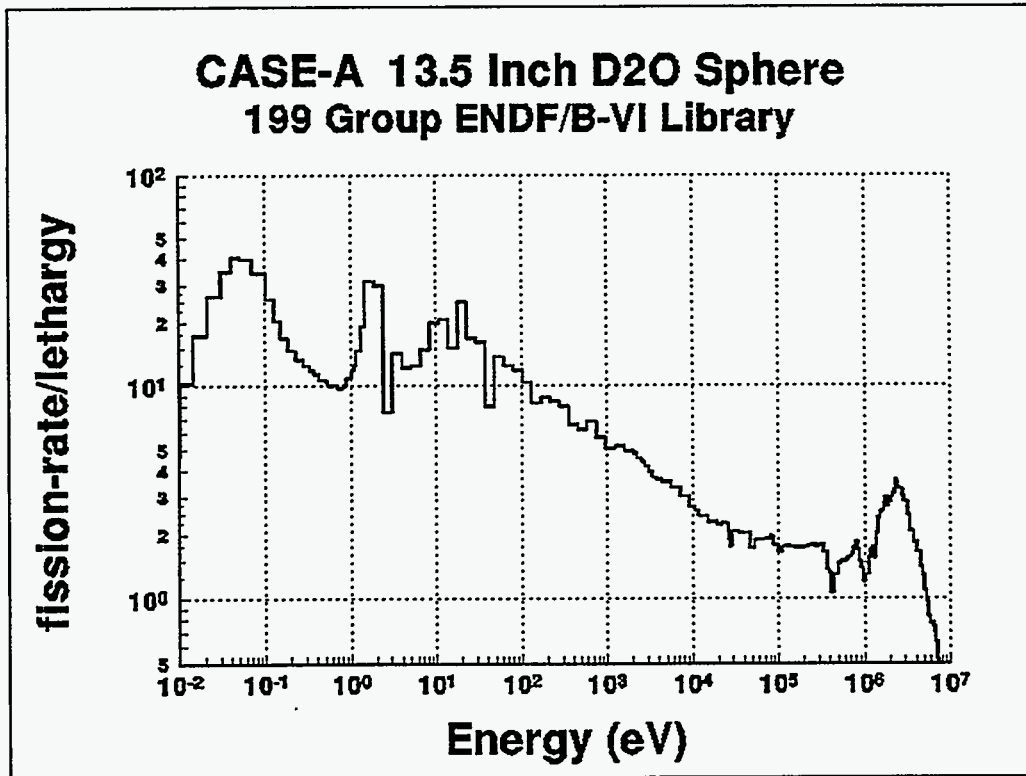
Fig. 4. Fission rate/lethargy for Case A.

fission-rate/lethargy

CASE-C Numerical Benchmark
199 Group ENDF/B-VI Library
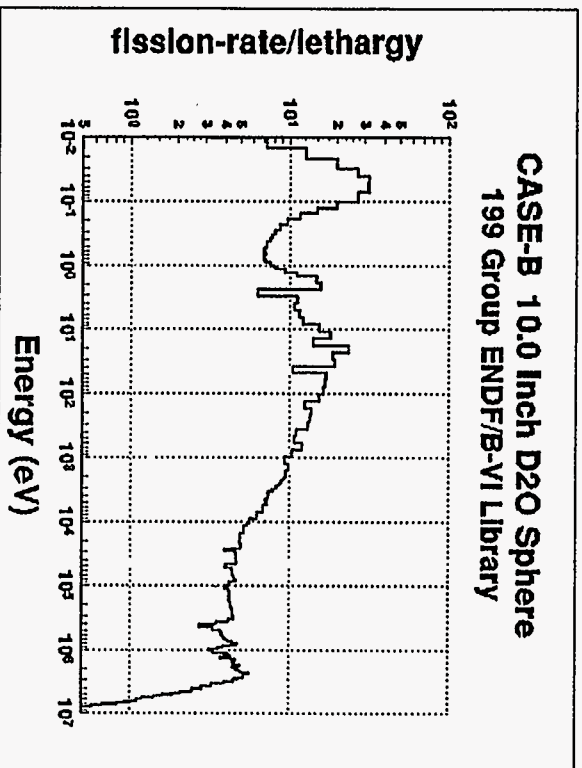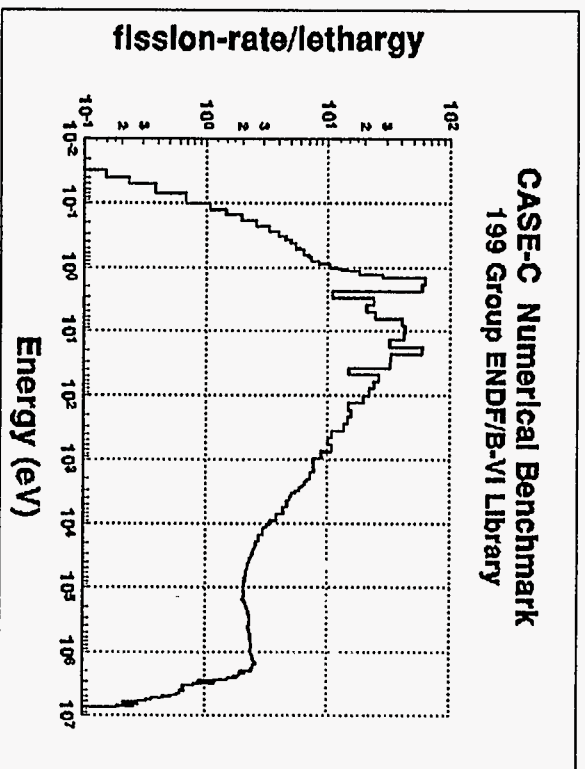
Fig. 6. Fission rate/lethargy for Case C.

fission-rate/lethargy

CASE-B 10.0 Inch D2O Sphere
199 Group ENDF/B-VI Library

Fig. 5. Fission rate/lethargy for Case B.

16
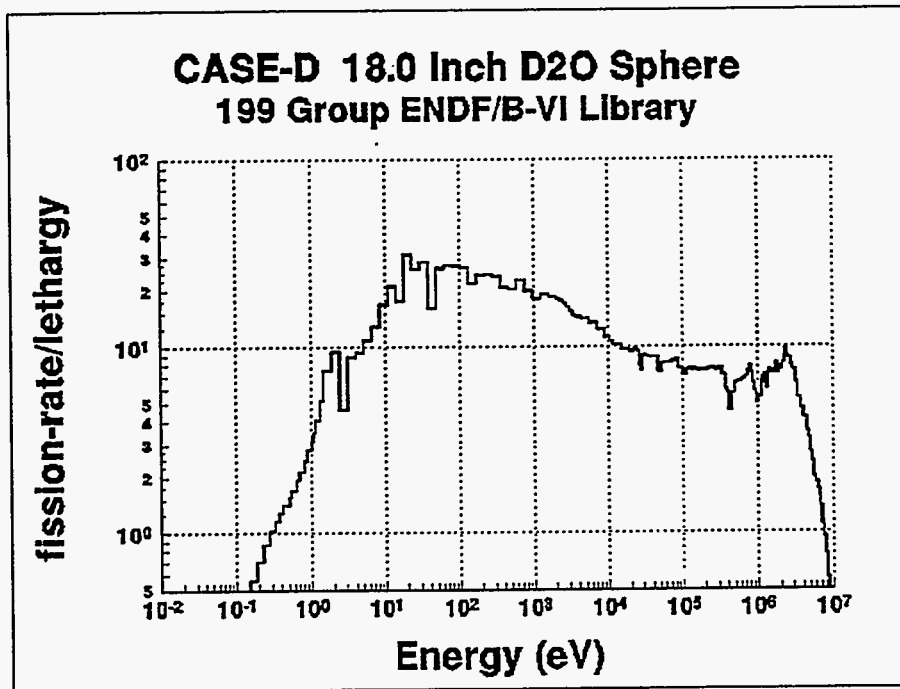
Fig. 7. Fission rate/lethargy for Case D.

We conclude that for some benchmarks with intermediate spectra, JENDL-3 and ENDF/B-VI will produce calculated k_{eff} values that are in good agreement. For other benchmarks, there are significant differences. As stated at the beginning of this section, it is not possible to determine which of the evaluations is better for spectrum peaking in the intermediate energy range; all we can do is determine relative differences between the two evaluations.

6. AD HOC ^{233}U EVALUATION

The results of calculations for the thermal benchmark experiments indicate that the ^{233}U JENDL-3 evaluation does an excellent job of predicting k_{eff} of systems in the thermal energy range; the average k_{eff} is 0.9995 (see Table 5). The ENDF/B-VI evaluation results are lower (Table 5). In the fast energy range, the ^{233}U ENDF/B-VI evaluation gives better results than the JENDL-3 evaluation. The average k_{eff} for the ten fast critical benchmark experiments using the JENDL-3 evaluation is 1.0112, while the average k_{eff} with ENDF/B-VI is 0.9980 (see Table 7). The ENDF/B-VI results are not totally satisfactory, however. The k_{eff} for the bare ^{233}U sphere (JEZEBEL-23) is only 0.9929 using ENDF/B-VI; a value closer to 1.0 is desirable.

A comparison of the fast cross sections in the ENDF/B-VI and JENDL-3 evaluations is given in Table 3. The inelastic, fission, and capture cross sections in the JENDL-3 evaluation are higher than the ENDF/B-VI cross sections. It seems feasible that a minor change to the JENDL-3 evaluation in the fast energy range will improve the fast benchmark results without adversely affecting the thermal benchmark results. It was decided to reduce the JENDL-3 fission cross section in the fast energy range. The ^{233}U fission cross section in the JENDL-3 evaluation was changed, as shown in Fig. 8. This is a uniform reduction of 2.0% between 0.1 and 3.6 MeV. The ad hoc JENDL-3 fission is compared with ENDF/B-VI in Fig. 9. The revised fission is lower between 0.1 and 0.9 MeV and about the same, or slightly higher, between 0.9 and 6 MeV. The elastic cross section was increased in the ad hoc JENDL-3 evaluation to offset the reduction in the fission cross section.

NJOY was used to generate 199-group cross sections based on the ad hoc ^{233}U JENDL-3 evaluation. SMILER was then used to produce an AMPX library, and this file was used in the ^{233}U benchmark calculations. Calculated k_{eff} values using these data are compared with the ENDF/B-VI and JENDL-3 values in Tables 11 and 12. The calculated k_{eff} values for the thermal benchmarks are almost unchanged from the original JENDL results. The calculated k_{eff} values for the fast benchmarks are greatly improved relative to both the ENDF/B-VI and JENDL-3 values given in Table 7. The calculated k_{eff} for the JEZEBEL-23 benchmark is 1.0007 compared to 0.9929 with ENDF/B-VI and 1.0125 with JENDL-3. The average k_{eff} for the reflected cases, not including the two tungsten reflected cases, is 0.9986. The calculated k_{eff} results for the bare and reflected cases using the ad hoc JENDL-3 evaluation are good. This is not the case for calculations using the ENDF/B-VI evaluation. It is also noted that the calculated k_{eff} for the ^{235}U, normal uranium, and beryllium reflected benchmarks are in good agreement and differ by only small amounts from the average value of 0.9986. The higher k_{eff} for the tungsten reflected cases appears to be due to problems with the tungsten cross sections or may possibly be due to problems with the specifications for those benchmarks. Using the ad hoc JENDL-3 evaluation, the average k_{eff} for all 16 benchmarks (fast and thermal) is 0.9999; these are excellent results and represent substantial improvement relative to either the ENDF/B-VI or JENDL-3 evaluations.

18

U-233 Fission Cross Section
JENDL-3 vs. AD HOC-REV
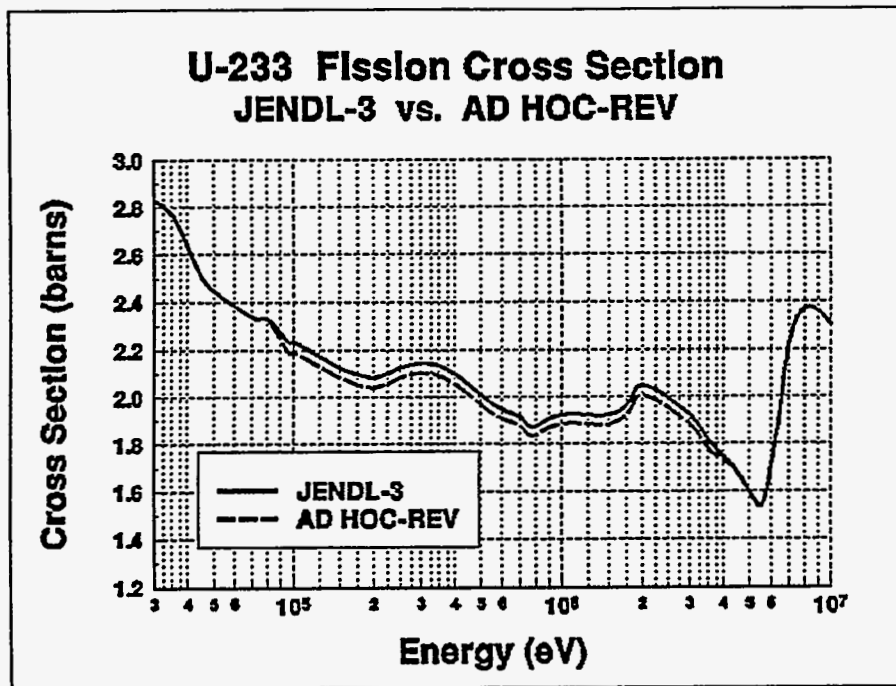
Fig. 8. Comparison of fission cross section for JENDL-3 and ad hoc JENDL.

U-233 Fission Cross Section
ENDF/B-VI vs. AD HOC-REV
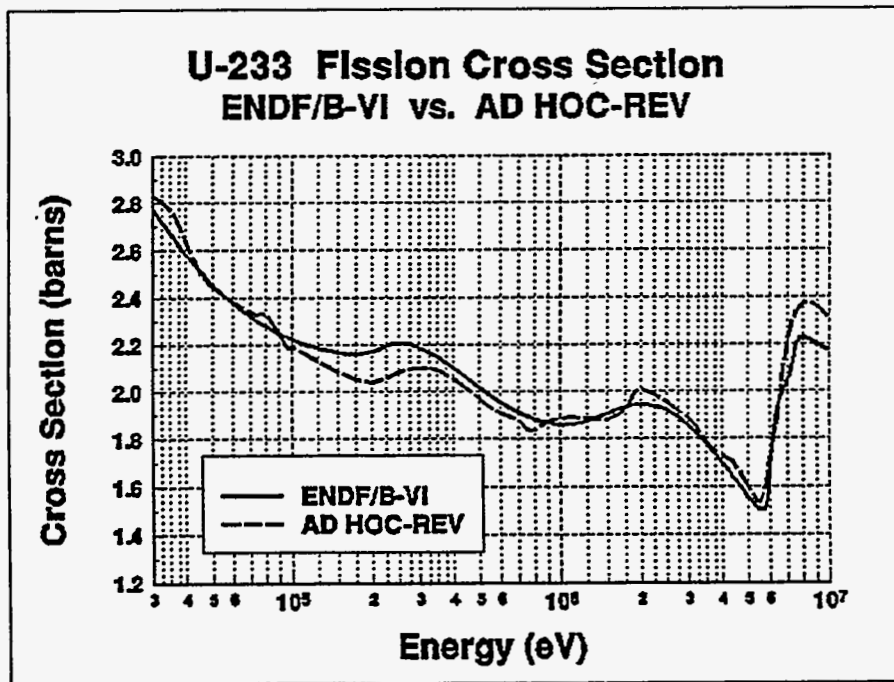
Fig. 9. Comparison of fission cross section for ENDF/B-VI and ad hoc JENDL.

19

Table 11. Result of calculations of the ORNL thermal benchmarks for the
199-group library with the ^{233}U ad hoc evaluation

Benchmark	ENDF/B	JENDL	AD HOC- REV
ORNL-5	0.9968	0.9997	0.9995
ORNL-6	0.9972	1.0002	1.0000
ORNL-7	0.9970	0.9999	0.9997
ORNL-8	0.9969	0.9999	0.9997
ORNL-9	0.9963	0.9993	0.9990
ORNL-11	0.9954	0.9980	0.9980
Average	0.9966	0.9995	0.9993

Table 12. Result of calculations of the fast benchmarks for the 199-group
library with the ^{233}U ad hoc evaluation

Benchmark	ENDF/B	JENDL	AD HOC-REV
^{233}U-MET-FAST-001 (JEZEBEL-23)	0.9929	1.0125	1.0007
^{233}U-MET-FAST-002-a	0.9952	1.0093	0.9989
^{233}U-MET-FAST-002-b	0.9975	1.0088	0.9995
^{233}U-MET-FAST-003-a	0.9958	1.0100	0.9988
^{233}U-MET-FAST-003-b	0.9971	1.0085	0.9976
^{233}U-MET-FAST-004-a	1.0027	1.0172	1.0068
^{233}U-MET-FAST-004-b	1.0061	1.0181	1.0057
^{233}U-MET-FAST-005-a	0.9949	1.0094	0.9980
^{233}U-MET-FAST-005-b	0.9974	1.0097	0.9988
FLATTOP-23	1.0004	1.0088	0.9985
Average	0.9980	1.0112	1.0003

It is essential that the revised ^{233}U fission cross section should be in good agreement with measured data. This has been investigated by examining the ^{233}U/^{235}U fission cross-section ratio. The ENDF/B-VI ^{235}U fission cross section was used, along with the new ^{233}U fission cross section. The JENDL-3 revised ^{233}U/^{235}U fission ratio is compared with the measured values from Kanda[17] in Figs. 10 and 11. The evaluated ratio is in good agreement with measured values. Based on this study, we conclude that the new ^{233}U fission cross section is reasonable.

A comparison of the ^{233}U/^{235}U fission reaction rate ratios for four fast benchmarks using ENDF/B-VI and JENDL-3 cross sections is given in Table 9. The calculated ratios using the new evaluation are compared with those using the other evaluations in Table 13. The calculated values using the ad hoc evaluation are in good agreement with the experimental values and with ENDF/B-VI values for the JEZEBEL, GODIVA, and FLATTOP-25 benchmarks. The calculated ratio for the BIGTEN benchmark is low relative to both the experimental value and the ENDF/B-VI result. We are currently unable to conclude whether this is due to a problem with the ^{233}U fission cross section or due to some other cause related to the BIGTEN benchmark.

Calculated values of the ^{238}U/^{235}U and ^{237}Np/^{235}U fission ratios using ENDF/B-VI, JENDL-3, and the ad hoc cross sections are compared in Table 14 for the JEZEBEL-23 and FLATTOP-23 benchmarks. These two benchmarks contain ^{233}U, while the ones given in Table 13 do not. The calculated values for the ^{237}Np/^{235}U fission ratio using all three evaluations are in good agreement and are also in agreement with measured values. The calculated values for the ^{238}U/^{235}U fission ratio using the ad hoc cross sections are lower than the corresponding ENDF/B-VI calculated values and are also low relative to the measured values. One important factor which influences the calculated ^{238}U/^{235}U fission ratio is the ^{233}U inelastic scattering cross section. The higher ^{233}U inelastic cross section in the JENDL-3 and ad hoc evaluations, relative to the ENDF/B-VI evaluation, appears to be the principal reason for the lower values of the calculated ^{238}U/^{235}U fission ratio using these evaluations, relative to the corresponding values using ENDF/B-VI.
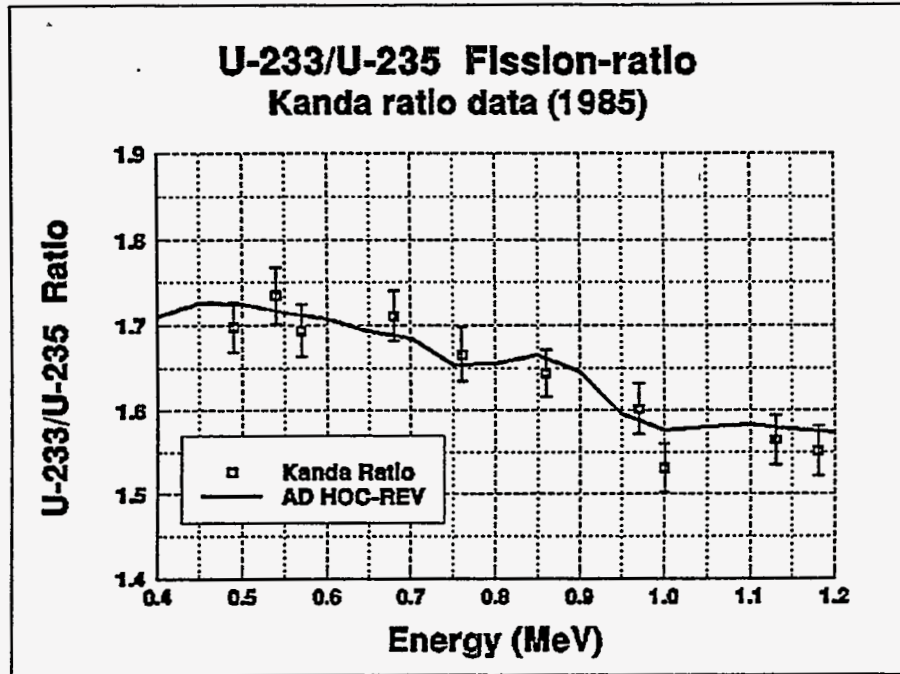
Fig. 10. Comparison of measured and evaluated $^{233}U/^{235}U$ fission cross-section ratio.
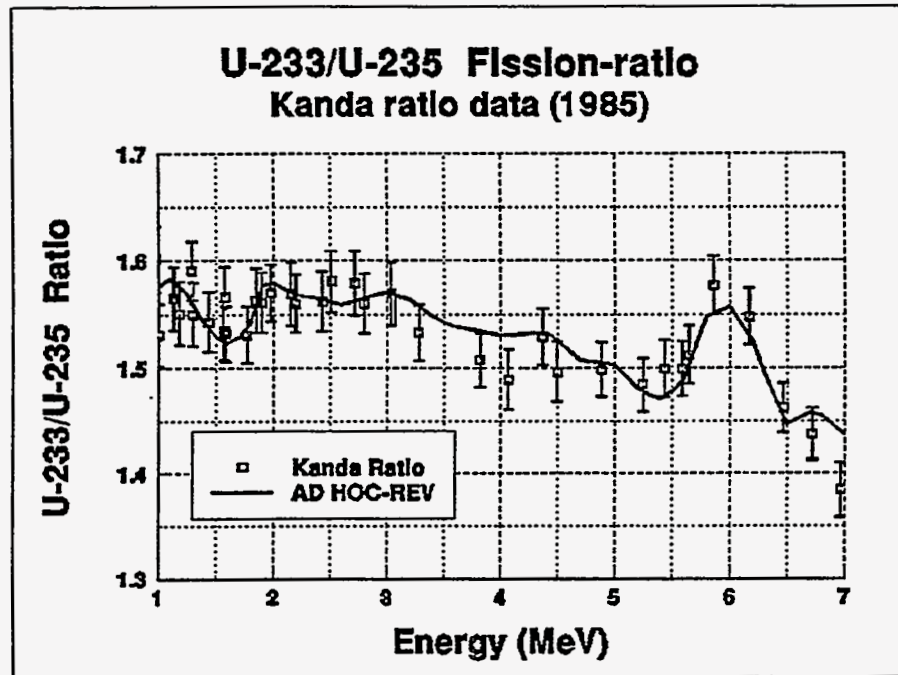
Fig. 11. Comparison of measured and evaluated $^{233}U/^{235}U$ fission cross-section ratio.

Table 13. Comparisons of $^{233}U/^{235}U$ fission central-reaction-rate ratios

Benchmark	Experiment	ENDF/B (C/E)	JENDL (C/E)	AD HOC-REV (C/E)
JEZEBEL	1.578±1.7%	1.000	1.016	0.998
GODIVA	1.590±1.9%	1.001	1.012	0.994
FLATTOP-25	1.595±1.9%	0.990	1.007	0.989
BIGTEN	1.580±1.9%	0.996	0.992	0.976

Table 14. Comparisons of $^{238}U/^{235}U$ and $^{237}Np/^{235}U$ fission central-reaction-rate ratios

Benchmark	Experiment	ENDF/B (C/E)	JENDL (C/E)	AD HOC-REV (C/E)
JEZEBEL-23				
$^{238}U/^{235}U$	0.213±1.1%	1.012	0.985	0.983
$^{237}Np/^{235}U$	0.977±1.6%	1.010	1.008	1.007
FLATTOP-23				
$^{238}U/^{235}U$	0.191±1.0%	0.998	0.981	0.977
$^{237}Np/^{235}U$	0.892±1.6%	1.013	1.014	1.012

7. CONCLUSIONS

In this study we have investigated the adequacy of the available ^{233}U cross-section data for benchmark calculations of experimental critical systems. An ad hoc ^{233}U cross-section evaluation, based on a modification of the JENDL-3 evaluation, was developed for test purposes.

Benchmark calculations of sixteen ^{233}U critical experiments, six thermal and ten fast, and four numerical benchmarks were performed. Calculations were done using the ENDF/B-VI, JENDL-3, and ad hoc JENDL-3 evaluations. In the ad hoc evaluation the fission cross section between 0.1 and 3.6 MeV was set to a value 2% lower than those given in JENDL-3. Using these values, excellent results for calculated k_{eff} values are obtained for both the thermal and fast benchmarks considered in this study. Results obtained with the ad hoc evaluation represent a big improvement relative to either the ENDF/B-VI or JENDL-3 evaluations. As discussed in Sect. 6, the ad hoc ^{233}U fission cross section is in agreement with the measured cross section, based on a comparison of the evaluated and measured ^{233}U/^{235}U fission ratio.

The lack of critical benchmark experiments with spectra peaking in the intermediate energy range is a serious limitation which prevents testing of the ^{233}U cross sections in this energy range. At the present time, measurements of ^{233}U cross sections from thermal to 600 eV are planned at the Oak Ridge Electron Linear Accelerator (ORELA). In addition, Los Alamos is planning to perform integral measurements on ^{233}U. These measurements will lead to more accurate ^{233}U data for use in applications which have specra in the intermediate energy range.

8. REFERENCES

1. ENDF/B-VI Summary Documentation, BNL-NCS-17541 [ENDF-201], 4th Edition, P. F. Rose, Ed., Brookhaven National Laboratory, October 1991.

2. Y. Kikuchi, "JENDL-3 Revision-2," *Nuclear Data for Science and Technology, Proc. of the International Conference*, ed., J. K Dickens, Oak Ridge National Laboratory, 1995.

3. N. M. Greene, J. W. Arwood, R. Q. Wright, and C. V. Parks, *The LAW Library—A Multigroup Cross-Section Library for Use in Radioactive Waste Analysis Calculations*, ORNL/TM-12370, Martin Marietta Energy Systems, Inc., Oak Ridge Natl. Lab., August 1994.

4. J. E. White, R. Q. Wright, D. T. Ingersoll, R. W. Roussin, N. M. Greene, and R. E. MacFarlane, "VITAMIN-B6: A Fine-Group Cross Section Library Based on ENDF/B-VI for Radiation Transport Applications," pp. 733-36 in *Nuclear Data for Science and Technology, Proc. of the International Conference*, ed., J. K Dickens, Oak Ridge National Laboratory, 1995; see also D. T. Ingersoll et al., *Production and Testing of the VITAMIN-B6 Fine Group and the BUGLE-93 Broad-Group Neutron/Photon Cross-Section Libraries Derived from ENDF/B-VI Nuclear Data*, NUREG/CR-6214 (ORNL-6795), U.S. Nuclear Regulatory Commission, January 1995.

5. L. M. Petrie and N. M. Greene, "XSDRNPM-S: A One-Dimensional Discrete Ordinates Code for Transport Analysis," Sect. F3 of *SCALE: A Modular Code System for Performing Standardized Computer Analyses for Licensing Evaluation*, NUREG/CR-0200, Rev. 4 (ORNL/NUREG/CSD-2R4), Vols. I, II, and III (April 1995). Available from Radiation Shielding Information Center at Oak Ridge National Laboratory as CCC-545.

6. R. E. MacFarlane and D. W. Muir, *The NJOY Nuclear Data Processing System*, Version 91, LA-12740-M, 1994.

7. N. M. Greene, W. E. Ford III, L. M. Petrie, and J. W. Arwood, *AMPX-77: A Modular Code System for Generating Coupled, Multigroup Neutron-Gamma Cross-Section Libraries from ENDF/B-IV and/or ENDF/B-V*, ORNL/CSD-283, Martin Marietta Energy Systems, Inc., Oak Ridge Natl. Lab., October 1992.

8. D. B. Adler and F. T. Adler, *Proceedings for the Conference on Breeding, Economics, and Safety in Large Fast Power Reactors*, ANL-6792, Argonne National Laboratory, October 7-10, 1963.

9. H. Derrien, "R-Matrix Analysis of Neutron Effective Total Cross Section, Fission Cross Section, and Capture Cross Section of ^{233}U in the Energy Range from Thermal to 150 eV," *Journal of Nucl. Sci. and Technol.* **31**, 379-97 (1994).

10. C. W. Reich and M. S. Moore, "Multilevel Formula for the Fission Process," *Phy. Rev.* **111**, 929 (1958).

11. N. M. Larson, *Update Users' Guide for SAMMY: Multilevel R-matrix Fits to Neutron Data Using Bayes' Equations*, ORNL/TM-97101/R1 (1985) and ORNL/TM-9179/R2 (1989), Martin Marietta Energy Systems, Inc., Oak Ridge Natl. Lab.

12. W. Kolar, G. Carraro, and G. Nastri, *Total Neutron Cross Section of ^{233}U from 0.7 to 320 eV*, Helsinki, Vol. I, 387 (1970); data Available on the NNDC/BNL Data Bank under Accession Number 20114.

13. National Nuclear Data Center, Brookhaven National Laboratory Associated Universities, Inc., Upton, Long Island, New York 11973.

14. *SCALE: A Modular Code System for Performing Standardized Computer Analyses for Licensing Evaluation*, NUREG/CR-0200, Rev. 4 (ORNL/NUREG/CSD-2R4), Vols. I, II, and III (April 1995). Available from Radiation Shielding Information Center at Oak Ridge National Laboratory as CCC-545.

15. *Cross Section Evaluation Working Group Benchmark Specifications*, BNL-19302 (ENDF-202), National Nuclear Data Center, Brookhaven National Lab., 1974.

16. A. D. Carlson, W. P. Poenitz, G. M. Hale, R. W. Peelle, D. C. Doddler, C. Y. Fu, and W. Manhart, *The ENDF/B-VI Neutron Cross Section Measurement Standards*, NISTIR 5177, National Institute of Standards and Technology, May 1993.

17. K. Kanda et al., "Measurement of Fast Neutron Induced Fission Cross Sections of ^{232}Th, ^{233}U, and ^{234}U Relative to ^{235}U," *Nuclear Data for Basic and Applied Science*, Vol. 1, Santa Fe, New Mexico (May 1985).

APPENDIX A

A.1. Listing of the NJOY Procedure to Process ^{233}U Cross Sections in the 238-Group Structure

```
cat > input233 << eof
0
6/
*reconr*
 21 22
*pendf tape for u-233, mat 9222, jendl evaluation*/
9222 3 0
.001 0. 7 /
*u-233, jendl evaluation*/
*processed by the njoy system*/
*R. Q. Wright & L. C. Leal 4-1-96*/
0/
*broadr*
22 23
9222 1 0 1 0.0
.001/
300.
0/
*unresr*
21 23 24
9222 1 7 1
300.
1.e10 1.e6 1.e5 1.e4 1.e3 100. 50.
0/
*thermr*
0 24 25
0 9222 8 1 1 0 1 221 0
300.
.01 3.0000
*groupr*
 21  25  0  26
 9222 1 0 4 5 1 7 1
*  u-233  jendl evaluation, mat 9222*/
300.
1.e10  1.e6 1.e5 1.e4 1.e3 1.e2  50.
238
  1.0000-5  1.0000-4  5.0000-4  7.5000-4  1.0000-3  1.2000-3
  1.5000-3  2.0000-3  2.5000-3  3.0000-3  4.0000-3  5.0000-3
  7.5000-3  1.0000-2  2.5300-2  3.0000-2  4.0000-2  5.0000-2
  6.0000-2  7.0000-2  8.0000-2  9.0000-2  1.0000-1  1.2500-1
  1.5000-1  1.7500-1  2.0000-1  2.2500-1  2.5000-1  2.7500-1
  3.0000-1  3.2500-1  3.5000-1  3.7500-1  4.0000-1  4.5000-1
  5.0000-1  5.5000-1  6.0000-1  6.2500-1  6.5000-1  7.0000-1
  7.5000-1  8.0000-1  8.5000-1  9.0000-1  9.2500-1  9.5000-1
  9.7500-1  1.0000+0  1.0100+0  1.0200+0  1.0300+0  1.0400+0
  1.0500+0  1.0600+0  1.0700+0  1.0800+0  1.0900+0  1.1000+0
  1.1100+0  1.1200+0  1.1300+0  1.1400+0  1.1500+0  1.1750+0
  1.2000+0  1.2250+0  1.2500+0  1.3000+0  1.3500+0  1.4000+0
  1.4500+0  1.5000+0  1.5900+0  1.6800+0  1.7700+0  1.8600+0
  1.9400+0  2.0000+0  2.1200+0  2.2100+0  2.3000+0  2.3800+0
  2.4700+0  2.5700+0  2.6700+0  2.7700+0  2.8700+0  2.9700+0
  3.0000+0  3.0500+0  3.1500+0  3.5000+0  3.7300+0  4.0000+0
```

```
4.7500+0 5.0000+0 5.4000+0 6.0000+0 6.2500+0 6.5000+0
6.7500+0 7.0000+0 7.1500+0 8.1000+0 9.1000+0 1.0000+1
1.1500+1 1.1900+1 1.2900+1 1.3750+1 1.4400+1 1.5100+1
1.6000+1 1.7000+1 1.8500+1 1.9000+1 2.0000+1 2.1000+1
2.2500+1 2.5000+1 2.7500+1 3.0000+1 3.1250+1 3.1750+1
3.3250+1 3.3750+1 3.4600+1 3.5500+1 3.7000+1 3.8000+1
3.9100+1 3.9600+1 4.1000+1 4.2400+1 4.4000+1 4.5200+1
4.7000+1 4.8300+1 4.9200+1 5.0600+1 5.2000+1 5.3400+1
5.9000+1 6.1000+1 6.5000+1 6.7500+1 7.2000+1 7.6000+1
8.0000+1 8.2000+1 9.0000+1 1.0000+2 1.0800+2 1.1500+2
1.1900+2 1.2200+2 1.8600+2 1.9250+2 2.0750+2 2.1000+2
2.4000+2 2.8500+2 3.0500+2 5.5000+2 6.7000+2 6.8300+2
9.5000+2 1.1500+3 1.5000+3 1.5500+3 1.8000+3 2.2000+3
2.2900+3 2.5800+3 3.0000+3 3.7400+3 3.9000+3 6.0000+3
8.0300+3 9.5000+3 1.3000+4 1.7000+4 2.5000+4 3.0000+4
4.5000+4 5.0000+4 5.2000+4 6.0000+4 7.3000+4 7.5000+4
8.2000+4 8.5000+4 1.0000+5 1.2830+5 1.5000+5 2.0000+5
2.7000+5 3.3000+5 4.0000+5 4.2000+5 4.4000+5 4.7000+5
4.9952+5 5.5000+5 5.7300+5 6.0000+5 6.7000+5 6.7900+5
7.5000+5 8.2000+5 8.6110+5 8.7500+5 9.0000+5 9.2000+5
1.0100+6 1.1000+6 1.2000+6 1.2500+6 1.3170+6 1.3560+6
1.4000+6 1.5000+6 1.8500+6 2.3540+6 2.4790+6 3.0000+6
4.3040+6 4.8000+6 6.4340+6 8.1873+6 1.0000+7 1.2840+7
1.3840+7 1.4550+7 1.5683+7 1.7333+7 2.0000+7
0.125 0.025 6.7400e+4 1.2730e+6
3/
3 221 *thrsct*/
3 251 *mubar*/
3 252 *xi*/
3 253 *gamma*/
3 452 *nubar*/
6/
6 221 *thrsct*/
0/
0/
*stop*
eof
/home/e5a/u233dir/xnjoyrsic < input233
echo 'njoy run is finished'
```

A.2. Listing of the NJOY Procedure to Process ^{233}U Cross Sections in the 199-Group Structure

```
cat > input233 << eof
0
6/
*reconr*
 21 22
*pendf tape for u-233, mat 9222, jendl evaluation*/
9222 3 0
.001 0. 7 /
*u-233, jendl evaluation*/
*processed by the njoy system*/
*R. Q. Wright & L. C. Leal 4-1-96*/
0/
*broadr*
22 23
9222 1 0 1 0.0
.001/
300.
0/
*unresr*
21 23 24
9222 1 7 1
300.
1.e10 1.e6 1.e5 1.e4 1.e3 100. 50.
```

28

```
0/
*thermr*
0 24 25
0 9222 8 1 1 0 1 221 0
300.
.01 3.0000
*groupr*
 21  25  0  26
 9222 1 0 4 5 1 7 1
* u-233  mod1  evaluation, mat 9222*/
300.
1.e10  1.e6  1.e5  1.e4  1.e3  1.e2  50.
199
1.0000e-05 5.0000e-04 2.0000e-03 5.0000e-03 1.0000e-02 1.4500e-02
2.1000e-02 3.0000e-02 4.0000e-02 5.0000e-02 7.0000e-02 1.0000e-01
1.2500e-01 1.5000e-01 1.8400e-01 2.2500e-01 2.7500e-01 3.2500e-01
3.6680e-01 4.1399e-01 5.0000e-01 5.3158e-01 6.2506e-01 6.8256e-01
8.0000e-01 8.7643e-01
1.0000e+00 1.0400e+00 1.0800e+00 1.1253e+00 1.3000e+00 1.4450e+00
1.8554e+00 2.3824e+00 3.0590e+00 3.9279e+00 5.0435e+00 6.4760e+00
8.3153e+00 1.0677e+01 1.3710e+01 1.7604e+01 2.2603e+01 2.9023e+01
3.7266e+01 4.7851e+01 6.1442e+01 7.8893e+01 1.0130e+02 1.3007e+02
1.6702e+02 2.1445e+02 2.7536e+02 3.5357e+02 4.5400e+02 5.8295e+02
7.4852e+02 9.6112e+02 1.2341e+03 1.5846e+03 2.0347e+03 2.2487e+03
2.4852e+03 2.6126e+03 2.7465e+03 3.0354e+03 3.3546e+03 3.7074e+03
4.3074e+03 5.5308e+03 7.1017e+03 9.1188e+03 1.0595e+04 1.1709e+04
1.5034e+04 1.9305e+04 2.1875e+04 2.3579e+04 2.4176e+04 2.4788e+04
2.6058e+04 2.7000e+04 2.8501e+04 3.1828e+04 3.4307e+04 4.0868e+04
4.6309e+04 5.2475e+04 5.6562e+04 6.7379e+04 7.1998e+04 7.9499e+04
8.2503e+04 8.6517e+04 9.8037e+04 1.1109e+05 1.1679e+05 1.2277e+05
1.2907e+05 1.3569e+05 1.4264e+05 1.4996e+05 1.5764e+05 1.6573e+05
1.7422e+05 1.8316e+05 1.9255e+05 2.0242e+05 2.1280e+05 2.2371e+05
2.3518e+05 2.4724e+05 2.7324e+05 2.8725e+05 2.9452e+05 2.9721e+05
2.9849e+05 3.0197e+05 3.3373e+05 3.6883e+05 3.8774e+05 4.0762e+05
4.5049e+05 4.9787e+05 5.2340e+05 5.5023e+05 5.7844e+05 6.0810e+05
6.3928e+05 6.7206e+05 7.0651e+05 7.4274e+05 7.8082e+05 8.2085e+05
8.6294e+05 9.0718e+05 9.6164e+05 1.0026e+06 1.1080e+06 1.1648e+06
1.2246e+06 1.2874e+06 1.3534e+06 1.4227e+06 1.4957e+06 1.5724e+06
1.6530e+06 1.7377e+06 1.8268e+06 1.9205e+06 2.0190e+06 2.1225e+06
2.2313e+06 2.3069e+06 2.3457e+06 2.3653e+06 2.3852e+06 2.4660e+06
2.5924e+06 2.7253e+06 2.8651e+06 3.0119e+06 3.1664e+06 3.3287e+06
3.6788e+06 4.0657e+06 4.4933e+06 4.7237e+06 4.9659e+06 5.2205e+06
5.4881e+06 5.7695e+06 6.0653e+06 6.3763e+06 6.5924e+06 6.7032e+06
7.0469e+06 7.4082e+06 7.7880e+06 8.1873e+06 8.6071e+06 9.0484e+06
9.5123e+06 1.0000e+07 1.0513e+07 1.1052e+07 1.1618e+07 1.2214e+07
1.2523e+07 1.2840e+07 1.3499e+07 1.3840e+07 1.4191e+07 1.4550e+07
1.4918e+07 1.5683e+07 1.6487e+07 1.6905e+07 1.7332e+07 1.9640e+07
0.125 0.025 8.2085e+5 1.2730e+6
3/
3 221 *thrsct*/
3 251 *mubar*/
3 252 *xi*/
3 253 *gamma*/
3 452 *nubar*/
6/
6 221 *thrsct*/
0/
0/
*stop*
eof
/home/e5a/u233dir/xnjoyrsic < input233
echo 'njoy run is finished'
```

APPENDIX B

B.1. CSASN Procedure to Execute XSDRNPM for ORNL5 Critical Benchmark

```
#csasn        parm=size=700000
 ornl-5 benchmark -- R. Q. Wright & L. C. Leal,  10-30-95
 199gr multiregion
 H  1  0.0  0.066360 end
 O  1  0.0  0.033607 end
 N  1  0.0  1.178-4  end
 U-233  1  0.0  4.328-5 end
 U-234  1  0.0  7.16-7 end
 U-235  1  0.0  1.80-8 end
 U-238  1  0.0  2.810-7 end
 TH-232 1  0.0  1.9641-7 end
 end comp
 spherical  vacuum  reflected  0.0 end
 1  34.595  noextermod
 end zone
end
#xsdrnpm
 ornl-5 benchmark, R. Q. Wright & L. C. Leal  10-10-95
-1$$ 700000  e
1$$ 3 2 40 1 0 1 8  8 3 1 1 10 35 3z
2$$ -1 5z -1 e   3$$  8z 5 1 e
5** 1.0-6  1.0-6  e  t
13$$ f1
14$$ 1001001 1008016 1007014 1092233 1092234 1092235
     1092238 1090232
15** 0.066360 0.033607 1.178-4 4.328-5 7.16-7 1.80-8
     2.81-7 1.9641-7  t
33** f1.0 t
35** 39i 0 34.595   36$$ 1 39r2
39$$ 1 1   40$$ f3
49$$ 1092233 1092238 1092233 1092238 1001001
50$$ 2r-18 3r-102  t
end
```

B.2. CSASN Procedure to Execute XSDRNPM for ORNL6 Critical Benchmark

```
#csasn        parm=size=700000
 ornl-6 benchmark -- R. Q. Wright & L. C. Leal,  10-30-95
 199gr multiregion
 H  1  0.0  0.066345  end
 O  1  0.0  0.033620  end
 N  1  0.0  1.224-4   end
 U-233  1  0.0  4.512-5 end
 U-234  1  0.0  7.44-7  end
 U-235  1  0.0  1.80-8  end
 U-238  1  0.0  2.910-7 end
 TH-232 1  0.0  2.0491-7 end
 B-10   1  0.0  2.6307-7 end
 end comp
 spherical  vacuum  reflected  0.0 end
 1  34.595  noextermod
 end zone
end
#xsdrnpm
 ornl-6 benchmark, R. Q. Wright & L. C. Leal  10-10-95
-1$$ 700000  e
1$$ 3 2 40 1 0 1 9  8 3 1 1 10 35 3z
2$$ -1 5z -1 e   3$$  8z 5 1 e
5** 1.0-6  1.0-6  e  t
```

```
13$$ fl
14$$ 1001001 1008016 1007014 1092233 1092234 1092235
     1092238 1090232 1005010
15** 0.066345 0.033620 1.224-4 4.512-5 7.44-7 1.80-8
     2.91-7 2.0491-7 2.6307-7 t
33** fl.0 t
35** 39i 0 34.595  36$$ 1 39r2
39$$ 1 1  40$$ f3
49$$ 1092233 1092238 1092233 1092238 1001001
50$$ 2r-18 3r-102 t
end
```

B.3. CSASN Procedure to Execute XSDRNPM for ORNL7 Critical Benchmark

```
#csasn        parm=size=700000
 ornl-7 benchmark -- R. Q. Wright and L. C. Leal, 10-31-95
 199gr multiregion
 H  1 0.0 0.066329 end
 O  1 0.0 0.033633 end
 N  1 0.0 1.274-4 end
 U-233  1 0.0 4.6798-5 end
 U-234  1 0.0 7.72-7 end
 U-235  1 0.0 1.80-8 end
 U-238  1 0.0 3.010-7 end
 TH-232 1 0.0 2.1333-7 end
 B-10   1 0.0 5.1230-7 end
 end comp  .
 spherical vacuum reflected 0.0 end
 1 34.595 noextermod
 end zone
end
#xsdrnpm
 ornl-7 benchmark, R. Q. Wright & L. C. Leal 10-10-95
-1$$ 700000 e
1$$ 3 2 40 1 0 1 9  8 3 1 10 35 3z
2$$ -1 5z -1 e  3$$ 8z 5 1 e
5** 1.0-6 1.0-6 e  t
13$$ fl
14$$ 1001001 1008016 1007014 1092233 1092234 1092235
     1092238 1090232 1005010
15** 0.066329 0.033633 1.274-4 4.6798-5 7.72-7 1.80-8
     3.01-7 2.1333-7 5.1230-7 t
33** fl.0 t
35** 39i 0 34.595  36$$ 1 39r2
39$$ 1 1  40$$ f3
49$$ 1092233 1092238 1092233 1092238 1001001
50$$ 2r-18 3r-102 t
end
```

B.4. CSASN Procedure to Execute XSDRNPM for ORNL8 Critical Benchmark

```
#csasn        parm=size=700000
 ornl-8 benchmark -- R. Q. Wright & L. C. Leal, 03-13-96
 199gr multiregion
 H  1 0.0 0.066315 end
 O  1 0.0 0.033646 end
 N  1 0.0 1.319-4 end
 U-233  1 0.0 4.8455-5 end
 U-234  1 0.0 8.01-7 end
 U-235  1 0.0 2.10-8 end
 U-238  1 0.0 3.110-7 end
 TH-232 1 0.0 2.2135-7 end
```

```
 B-10   1  0.0  7.5757-7  end
 end comp
 spherical  vacuum  reflected  0.0  end
 1  34.595  noextermod
 end zone
end
#xsdrnpm
 ornl-8 benchmark, R. Q. Wright & L. C. Leal  10-10-95
 -1$$  700000  e
 1$$  3 2 40 1 0 1 9  8 3 1 10 35 3z
 2$$  -1 5z -1 e  3$$  8z 5 1 e
 5**  1.0-6  1.0-6  e  t
 13$$  f1
 14$$  1001001  1008016  1007014  1092233  1092234  1092235
      1092238  1090232  1005010
 15**  0.066315  0.033646  1.319-4  4.8455-5  8.01-7  2.10-8
      3.11-7  2.2135-7  7.5757-7  t
 33**  f1.0  t
 35**  39i 0 34.595  36$$  1 39r2
 39$$  1 1  40$$  f3
 49$$  1092233 1092238 1092233 1092238 1001001
 50$$  2r-18  3r-102  t
 end
```

B.5. CSASN Procedure to Execute XSDRNPM for ORNL9 Critical Benchmark

```
#csasn        parm=size=700000
 ornl-9 benchmark -- R. Q. Wright & L. C. Leal,  03-13-96
 199gr multiregion
 H   1  0.0  0.066300  end
 O   1  0.0  0.033657  end
 N   1  0.0  1.363-4   end
 U-233  1  0.0  5.0066-5  end
 U-234  1  0.0  8.27-7  end
 U-235  1  0.0  2.10-8  end
 U-238  1  0.0  3.270-7  end
 TH-232  1  0.0  2.2693-7  end
 B-10   1  0.0  1.0048-6  end
 end comp
 spherical  vacuum  reflected  0.0  end
 1  34.595  noextermod
 end zone
end
#xsdrnpm
 ornl-9 benchmark, R. Q. Wright & L. C. Leal  10-10-95
 -1$$  700000  e
 1$$  3 2 40 1 0 1 9  8 3 1 10 35 3z
 2$$  -1 5z -1 e  3$$  8z 5 1 e
 5**  1.0-6  1.0-6  e  t
 13$$  f1
 14$$  1001001  1008016  1007014  1092233  1092234  1092235
      1092238  1090232  1005010
 15**  0.066300  0.033657  1.363-4  5.0066-5  8.27-7  2.10-8
      3.27-7  2.2693-7  1.0048-6  t
 33**  f1.0  t
 35**  39i 0 34.595  36$$  1 39r2
 39$$  1 1  40$$  f3
 49$$  1092233 1092238 1092233 1092238 1001001
 50$$  2r-18  3r-102  t
 end
```

B.6. CSASN Procedure to Execute XSDRNPM for ORNL11 Critical Benchmark

```
#csasn        parm=size=700000
 ornl-11 benchmark – R. Q. Wright & L. C. Leal,  10-31-95
 199gr multiregion
 H   1  0.0  0.066467  end
 O   1  0.0  0.033525  end
 N   1  0.0  7.530-5   end
 U-233  1  0.0  3.346-5  end
 U-234  1  0.0  5.25-7  end
 U-235  1  0.0  1.00-8  end
 U-238  1  0.0  2.560-7  end
 TH-232  1  0.0  1.4757-7  end
 end comp
 spherical  vacuum  reflected  0.0  end
 1  61.011  noextermod
 end zone
 end
 #xsdrnpm
 ornl-11 benchmark, R. Q. Wright & L. C. Leal  10-10-95
 -1$$ 700000  e
 1$$  3 2 40 1 0 1 8  8 3 1 10 70 3z
 2$$ -1 5z -1  e   3$$  8z 5 1 e
 5**  1.0-6  1.0-6  e   t
 13$$ f1
 14$$  1001001  1008016  1007014  1092233  1092234  1092235
      1092238  1090232
 15**  0.066467  0.033525  7.530-5  3.346-5  5.25-7  1.00-8
      2.56-7  1.4757-7   t
 33**  f1.0  t
 35**  39i 0 61.011   36$$  1 39r2
 39$$  1 1   40$$  f3
 49$$  1092233 1092238 1092233 1092238 1001001
 50$$  2r-18  3r-102   t
 end
```

```
#xsdrnpm
 u23nu10 benchmark, 199-grp cross sections, 06-28-95
1$$  3 3 60 1 0 2 8 16 3 1 10 25 3z
2$$ -2 0 0 e  3$$ 8z 5 1 e  t
13$$  6r1 2r2
14$$  1093237 1094239 1092233 1092234 1092235 1092238
     2092235 2092238
15**  2r1-15  4.7253-2  5.2705-4  1.0-15  3.2975-4
     3.4902-4  4.7518-2  t
33**  f1.0  t
35**  39i 0 19i 5.0444  7.3456   36$$  1 39r2 20r3
39$$  1 1 2   40$$  f3
49$$  1093237 1094239 1092233 1092235 1092238
50$$  5r-18  t
end
```

C.5. CSASN Procedure to Execute XSDRNPM for [233]U-MET-FAST-003-b Critical Benchmark

```
#csasn
 u23kg76 benchmark -- R. Q. Wright & L. C. Leal, 06-19-95
 199gr multiregion
 np-237  1  0.0  1.0-15  end
 pu-239  1  0.0  1.0-15  end
 u-235   1  0.0  1.0-15  end
 u-233   1  0.0  4.7312-2  end
 u-234   1  0.0  5.2770-4  end
 u-238   1  0.0  3.3015-4  end
 u-235   2  0.0  4.4892-2  end
 u-238   2  0.0  3.2340-3  end
 end comp
 spherical  vacuum  reflected  0.0  end
 1  4.5999  noextermod  2  6.5887  noextermod
 end zone
 moredata collapse  end
end
#xsdrnpm
 u23kg76 benchmark, 199-grp cross sections, 06-19-95
1$$  3 3 60 1 0 2 8 16 3 1 10 25 3z
2$$ -2 0 0 e  3$$ 8z 5 1 e  t
13$$  6r1 2r2
14$$  1093237 1094239 1092233 1092234 1092235 1092238
     2092235 2092238
15**  2r1-15  4.7312-2  5.2770-4  1.0-15  3.3015-4
     4.4892-2  3.2340-3  t
33**  f1.0  t
35**  39i 0 19i 4.5999  6.5887   36$$  1 39r2 20r3
39$$  1 1 2   40$$  f3
49$$  1093237 1094239 1092233 1092235 1092238
50$$  5r-18  t
end
```

C.6. CSASN Procedure to Execute XSDRNPM for [233]U-MET-FAST-004-a Critical Benchmark

```
#csasn
 u23w10 benchmark -- R. Q. Wright & L. C. Leal, 06-29-95
 199gr multiregion
 np-237  1  0.0  1.0-15  end
 pu-239  1  0.0  1.0-15  end
 u-235   1  0.0  1.0-15  end
 u-233   1  0.0  4.7253-2  end
 u-234   1  0.0  5.2705-4  end
```

```
u-238   1  0.0  3.2975-4  end
zr      2  0.0  7.9528-4  end
ni      2  0.0  9.7124-3  end
cu      2  0.0  4.0774-3  end
w       2  0.0  5.1468-2  end
end comp
spherical  vacuum  reflected  0.0  end
1  5.0444  noextermod  2  7.4828  noextermod
end zone
moredata collapse  end
end
#xsdrnpm
 u23w10 benchmark, 199-grp cross sections, 06-29-95
1$$  3 3 60 1 0 2 10 16 3 1 10 25 3z
2$$  -2 0 0 e  3$$  8z 5 1 e  t
13$$  6r1 4r2
14$$  1093237 1094239 1092233 1092234 1092235 1092238
      2028000  2029000  2040000  2074000
15**  2r1-15  4.7253-2  5.2705-4  1.0-15  3.2975-4
      9.7124-3  4.0774-3  7.9528-4  5.1468-2  t
33**  f1.0  t
35**  39i 0 19i 5.0444  7.4828   36$$  1 39r2 20r3
39$$  1 1 2  40$$  f3
49$$  1093237 1094239 1092233 1092235 1092238
50$$  5r-18  t
end
```

C.7. CSASN Procedure to Execute XSDRNPM for [233]U-MET-FAST-004-b Critical Benchmark

```
#csasn
 u23w76 benchmark -- R. Q. Wright & L. C. Leal, 06-28-95
 199gr multiregion
np-237  1  0.0  1.0-15  end
pu-239  1  0.0  1.0-15  end
u-235   1  0.0  1.0-15  end
u-233   1  0.0  4.7312-2  end
u-234   1  0.0  5.2770-4  end
u-238   1  0.0  3.3015-4  end
zr      2  0.0  7.9528-4  end
ni      2  0.0  9.7124-3  end
cu      2  0:0  4.0774-3  end
w       2  0.0  5.1468-2  end
end comp
spherical  vacuum  reflected  0.0  end
1  4.5999  noextermod  2  10.3911  noextermod
end zone
moredata collapse  end
end
#xsdrnpm
 u23w76 benchmark, 199-grp cross sections, 06-28-95
1$$  3 3 80 1 0 2 10 16 3 1 10 25 3z
2$$  -2 0 0 e  3$$  8z 5 1 e  t
13$$  6r1 4r2
14$$  1093237 1094239 1092233 1092234 1092235 1092238
      2028000  2029000  2040000  2074000
15**  2r1-15  4.7312-2  5.2770-4  1.0-15  3.3015-4
      9.7124-3  4.0774-3  7.9528-4  5.1468-2  t
33**  f1.0  t
35**  39i 0 39i 4.5999  10.3911   36$$  1 39r2 40r3
39$$  1 1 2  40$$  f3
49$$  1093237 1094239 1092233 1092235 1092238
50$$  5r-18  t
end
```

38

C.8. CSASN Procedure to Execute XSDRNPM for ²³³U-MET-FAST-005-a Critical Benchmark

```
#csasn        parm=size=700000
u23be76 benchmark -- R. Q. Wright & L. C. Leal,  03-21-96
199gr multiregion
np-237  1  0.0  1.0-15  end
pu-239  1  0.0  1.0-15  end
u-235   1  0.0  1.0-15  end
u-233   1  0.0  4.7312-2  end
u-234   1  0.0  5.2770-4  end
u-238   1  0.0  3.3015-4  end
bebound   2  0.0  1.1984-1  end
o-16   2  0.0  1.3776-3  end
end comp
spherical  vacuum  reflected  0.0  end
1  4.5999  noextermod  2  8.7960  noextermod
end zone
end
#xsdrnpm
u23w76 benchmark, 199-grp cross sections, 03-21-96
-1$$  700000  e
1$$  3 3 90 1 0 2  8 48 3 1 10 25 3z
2$$ -2  5z -1  e   3$$  8z 5 1 e
5**  1.0-6  1.0-6  e   t
13$$  6r1 2r2
14$$  1093237 1094239 1092233 1092234 1092235 1092238
     2004309  2008016
15**  2r1-15  4.7312-2  5.2770-4  1.0-15  3.3015-4
     1.19840-1  1.37760-3  t
33**  f1.0  t
35**  54i 0 34i 4.5999  8.7960   36$$  1 54r2 35r3
39$$  1 1 2   40$$  f3
49$$  1093237 1094239 1092233 1092235 1092238
50$$  5r-18  t
end
```

C.9. CSASN Procedure to Execute XSDRNPM for ²³³U-MET-FAST-005-b Critical Benchmark

```
#csasn        parm=size=700000
u23be76 benchmark -- R. Q. Wright & L. C. Leal,  03-21-96
199gr multiregion
np-237  1  0.0  1.0-15  end
pu-239  1  0.0  1.0-15  end
u-235   1  0.0  1.0-15  end
u-233   1  0.0  4.7312-2  end
u-234   1  0.0  5.2770-4  end
u-238   1  0.0  3.3015-4  end
bebound   2  0.0  1.1984-1  end
o-16   2  0.0  1.3776-3  end
end comp
spherical  vacuum  reflected  0.0  end
1  4.5999  noextermod  2  8.7960  noextermod
end zone
end
#xsdrnpm
u23w76 benchmark, 199-grp cross sections, 03-21-96
-1$$  700000  e
1$$  3 3 90 1 0 2  8 48 3 1 10 25 3z
2$$ -2  5z -1  e   3$$  8z 5 1 e
5**  1.0-6  1.0-6  e   t
13$$  6r1 2r2
14$$  1093237 1094239 1092233 1092234 1092235 1092238
     2004309  2008016
```

```
15**  2r1-15  4.7312-2  5.2770-4  1.0-15  3.3015-4
      1.19840-1  1.37760-3   t
33**  f1.0  t
35**  54i 0 34i 4.5999  8.7960   36$$  1 54r2 35r3
39$$  1 1 2   40$$  f3
49$$  1093237 1094239 1092233 1092235 1092238
50$$  5r-18   t
end
```

C.10. CSASN Procedure to Execute XSDRNPM for FLATTOP-23 Critical Benchmark

```
#csasn        parm=size=700000
 flattop-23 benchmark -- R. Q. Wright and L. C. Leal,  11-30-93
 199gr multiregion
 u-233   1  0.0  4.6710-2  end
 np-237  1  0.0  1.0-15  end
 pu-239  1  0.0  1.0-15  end
 u-234   1  0.0  5.8772-4  end
 u-235   1  0.0  1.4158-5  end
 u-238   1  0.0  2.7959-4  end
 u-235   2  0.0  3.5050-4  end
 u-238   2  0.0  4.7717-2  end
 end comp
 spherical  vacuum  reflected  0.0  end
 1  4.2058  noextermod  2  24.1194  noextermod
 end zone
 moredata collapse  end
end
#xsdrnpm
 flattop-23 benchmark,  199-grp cross sections,  11-30-93
1$$  3 3 62 1 0 2 8 16 3 1 10 25 3z
2$$  -2  5z -1 e  3$$  8z  6 1 e
5**  1.0-6  1.0-6  e  t
13$$  6r1 2r2
14$$  1092233  1093237  1094239  1092234  1092235  1092238
     2092235  2092238
15**  4.6710-2  2r1-15  5.8772-4  1.4158-5  2.7959-4
     3.5050-4  4.7712-2  t
33**  f1.0  t
35**  39i 0 2i 4.2058  18i 4.610  24.1194
36$$  1 39r2 22r3
39$$  1 1 2   40$$  f3
49$$  1092233  1093237  1094239  1092235  1092238  1092238
50$$  5r-18  -102  t
end
```

APPENDIX D

D.1. CSASN Procedure to Execute XSDRNPM for CASE A Numerical Benchmark

```
#csasn       parm=size=600000
 d2ox-1      13.5 in sphere, R. Q. Wright & L. C. Leal  01-10-96
199gr multiregion
H      1 0.0 1.78490-4 end
D      1 0.0 5.93180-2 end
O      1 0.0 3.34610-2 end
F      1 0.0 3.71290-3 end
U-233  1 0.0 5.38380-4 end
U-234  1 0.0 8.25000-6 end
U-235  1 0.0 4.10000-7 end
U-238  1 0.0 1.30945-3 end
SI     2 0.0 1.69820-3 end
CR-50  2 0.0 7.17402-4 end
CR-52  2 0.0 1.38346-2 end
CR-53  2 0.0 1.56854-3 end
CR-54  2 0.0 3.90485-4 end
MN     2 0.0 1.73630-3 end
FE-54  2 0.0 3.50194-3 end
FE-56  2 0.0 5.44404-2 end
FE-57  2 0.0 1.24646-3 end
FE-58  2 0.0 1.66194-4 end
NI-58  2 0.0 5.27065-3 end
NI-60  2 0.0 2.01500-3 end
NI-61  2 0.0 8.72394-5 end
NI-62  2 0.0 2.77159-4 end
NI-64  2 0.0 7.02547-5 end
H      3 0.0 3.98860-4 end
D      3 0.0 6.60780-2 end
O      3 0.0 3.32380-2 end
end comp
spherical  vacuum  reflected  0.0 end
 1 17.088 oneextermod  2 17.189 oneextermod  3 44.367 noextermod
end zone
end
=xsdrnpm
 k-calculation and reaction rates for d2ox-1 sphere,  01-10-96
-1$$  700000
1$$ 3 4 53 1 0 3 26 16 3 1 10 40 3z
2$$ -2 0 1 3z -1 3z 3$$ 1 7z 12 1 e
4$$  0  5  0  -2  e
5** 1.0-6  1.0-6  e   t
13$$ 8r1 15r2 3r3
14$$
 1001001  1001002  1008016  1009019  1092233  1092234
 1092235  1092238  2014000
 2024050  2024052  2024053  2024054  2025055
 2026054  2026056  2026057  2026058
 2028058  2028060  2028061  2028062  2028064
 3001001  3001002  3008016
15** 1.78490-4  5.93180-2  3.34610-2  3.71290-3
      5.38380-4  8.25000-6  4.10000-7
      1.30945-3  1.69820-3
      7.17402-4  1.38346-2  1.56854-3  3.90485-4  1.73630-3
      3.50194-3  5.44404-2  1.24646-3  1.66194-4
      5.27065-3  2.01500-3  8.72394-5  2.77159-4  7.02547-5
      3.98860-4  6.60780-2  3.32380-2   t
33## f1.0 t
35**
 15i 0 16 2i 16.5 17.088 17.189 2i 17.5 24i 19 44 1i 44.367
 44.621
36$$ 20r1 2 30r3 4 4
39$$ 1 2 3 2 40$$ f3
```

```
49$$ 3r1092233 3r1092234 3r1092235 3r1092238
50$$ -101 -102 -18 3q3
51$$  16r1  50r2  64r3  47r4  22r5   t
end
```

C.2. CSASN Procedure to Execute XSDRNPM for CASE B Numerical Benchmark

```
#csasn        parm=size=600000
 d2ox-1      10.0 in sphere, R. Q. Wright & L. C. Leal  04-02-96
199gr multiregion
H     1 0.0 1.78490-4 end
D     1 0.0 5.93180-2 end
O     1 0.0 3.34610-2 end
F     1 0.0 3.71290-3 end
U-233  1 0.0 1.70800-3 end
U-234  1 0.0 8.25000-6 end
U-235  1 0.0 4.10000-7 end
U-238  1 0.0 1.39830-4 end
SI    2 0.0 1.69820-3 end
CR-50  2 0.0 7.17402-4 end
CR-52  2 0.0 1.38346-2 end
CR-53  2 0.0 1.56854-3 end
CR-54  2 0.0 3.90485-4 end
MN    2 0.0 1.73630-3 end
FE-54  2 0.0 3.50194-3 end
FE-56  2 0.0 5.44404-2 end
FE-57  2 0.0 1.24646-3 end
FE-58  2 0.0 1.66194-4 end
NI-58  2 0.0 5.27065-3 end
NI-60  2 0.0 2.01500-3 end
NI-61  2 0.0 8.72394-5 end
NI-62  2 0.0 2.77159-4 end
NI-64  2 0.0 7.02547-5 end
H     3 0.0 3.98860-4 end
D     3 0.0 6.60780-2 end
O     3 0.0 3.32380-2 end
end comp
spherical  vacuum  reflected  0.0 end
 1 12.700 oneextermod  2 12.801 oneextermod  3 39.979 noextermod
end zone
end
=xsdrnpm
 k-calculation and reaction rates for d2ox-1 sphere,  04-02-96
-1$$  700000
1$$ 3 4 53 1 0 3 26 16 3 1 10 40 3z
2$$ -2 0 1 3z -1 3z 3$$ 1 7z 12 1 e
4$$  0  5  0  -2  e
5**  1.0-6  1.0-6  e   t
13$$ 8r1 15r2 3r3
14$$
 1001001  1001002  1008016  1009019  1092233  1092234
 1092235  1092238  2014000
 2024050  2024052  2024053  2024054  2025055
 2026054  2026056  2026057  2026058
 2028058  2028060  2028061  2028062  2028064
 3001001  3001002  3008016
15**  1.78490-4  5.93180-2  3.34610-2  3.71290-3
     1.70800-3  8.25000-6  4.10000-7
     1.39830-4  1.69820-3
     7.17402-4  1.38346-2  1.56854-3  3.90485-4  1.73630-3
     3.50194-3  5.44404-2  1.24646-3  1.66194-4
     5.27065-3  2.01500-3  8.72394-5  2.77159-4  7.02547-5
     3.98860-4  6.60780-2  3.32380-2   t
33## f1.0 t
35**
 15i 0 11.7 2i 12.2 12.700 12.801 2i 13.1 24i 14.6 39.6 1i 39.979
```

42

```
 40.233
36$$ 20r1 2 30r3 4 4
39$$ 1 2 3 2 40$$ f3
49$$ 3r1092233 3r1092234 3r1092235 3r1092238
50$$ -101 -102 -18 3q3
51$$ 16r1 50r2 64r3 47r4 22r5  t
end
```

C.3. CSASN Procedure to Execute XSDRNPM for CASE C Numerical Benchmark

```
#csasn
 hiss(u233) benchmark -- R. Q. Wright & L. C. Leal, 04-29-96
 199grp infh
 u-234 1 0 3.12000-6 end
 u-233 1 0 9.80530-5 end
 u-236 1 0 4.26700-7 end
 u-238 1 0 1.71900-5 end
 h  1 0 1.12600-4 end
 boron 1 2.058826-3 end
 c-graphite 1 0 7.56500-2 end
 o  1 0 1.65000-3 end
 ca  1 0 5.6970-4 end
 end comp
 end
#xsdrnpm
 hiss(u233) benchmark, 199-grp cross sections,  04-29-96
 1$$ 0 1 1 1 1 1 10 8 3 1 20 25 25 0 0
 2$$ -2 0 1 e
 3$$ 1 5r0 2 0 8 0 0 0
 4$$ 0 5 0 -2 e t
 13$$ 10r1
 14$$ 1092234 1092233 1092236 1092238 1001001 1005010 1005011
     1006312 1008016 1020000
 15** 3.1200-6 9.8053-5 4.2670-7 1.7190-5 1.1260-4
     5.74538-5 2.33246-4 7.5650-2 1.650-3 5.6970-4   t
 33** f1.0 t
 35** 0.0  10.0
 36$$ 1
 39$$ 1  40$$ f3  46$$ f0
 49$$ 1092235 1092238 1092235 1092238 1001001 1005010
     1005011 1020000
 50$$ 2r-18 2r-102 4r-101
 51$$ 16r1 50r2 64r3 47r4 22r5  t
 end
```

C.4. CSASN Procedure to Execute XSDRNPM for CASE D Numerical Benchmark

```
#csasn     parm=(size=600000)
 u-233  case-d  26.7 cm sphere, R. Q. Wright & L. C. Leal, 08-27-96
 199gr multiregion
 H    1 0.0 1.78490-4 end
 D    1 0.0 5.93180-2 end
 O    1 0.0 3.34610-2 end
 F    1 0.0 3.71290-3 end
 U-235 1 0.0 1.0000-20 end
 U-234 1 0.0 2.04210-5 end
 U-233 1 0.0 1.82342-3 end
 U-238 1 0.0 1.26420-5 end
 al    2 0.0 5.94690-2 end
 end comp
 spherical  vacuum  reflected  0.0 end
 1 22.900 oneextermod  2 23.300 noextermod
 end zone
 end
 =xsdrnpm
  k-calculation and reaction rates for case #d sphere,  08-27-96
```

```
-1$$ 600000
1$$ 3 2 74 1 0 2 9 16 3 1 10 40 3z
2$$ -2 5z -1 3z   3$$ 8z 12 1  e
5** 1.0-6  1.0-6 e  t
13$$ 8r1  2
14$$
 1001001  1001002  1008016  1009019  1092233  1092234
 1092235  1092238  2013027
15** 1.78490-4 5.93180-2 3.34610-2 3.71290-3
     1.82342-3 2.04210-5 1.0000-20
     1.26420-5 5.94690-2  t
33## f1.0 t
35**
 27i 0  41i 12.0 3i 22.9 23.3
36$$ 70r1 4r2
39$$ 1 2 40$$ f3
49$$ 3r1092233 3r1092234 3r1092235 3r1092238
50$$ -101 -102 -18 3q3
 t
end
```

INTERNAL DISTRIBUTION

1.	B. L. Broadhead	19.	L. F. Norris
2.	M. D. DeHart	20.	J. V. Pace
3.	F. Difillipo	21.	C. V. Parks
4.	K. R. Elam	22.	R. T. Primm, III
5.	C. W. Forsberg	23.	R. W. Roussin
6.	N. M. Greene	24.	R. M. Westfall
7.	D. M. Hetrick	25.	J. E. White
8.	C. M. Hopper	26.	B. A. Worley
9.	D. T. Ingersoll	27-31.	R. Q. Wright
10.	W. C. Jordan	32-33.	Laboratory Records Dept.
11.	M. A. Kuliasha	34.	Laboratory Records, ORNL-RC
12.	N. M. Larson	35.	Y-12 Technical Library
13-17.	L. C. Leal	36.	Central Research Library
18.	B. D. Murphy	37.	ORNL Patent Section

EXTERNAL DISTRIBUTION

38. J. Burke, Rensselaer Polytechnic Institute, Troy, NY 12180-3590

39. D. Cabrilla, U.S. Department of Energy, EM-23, 1000 Independence Avenue, Washington DC 20585-0002

40. D. E. Carlson, Reactor and Plant System Branch, Division of System Research, Office of Nuclear Regulatory Research, U.S. Nuclear Regulatory Commission, MS 06-G22, 11555 Rockville Pike, Rockville, MD 20852

41. R. L. Dintaman, U.S. Department of Energy, DP-13, Washington, DC 20585

42. C. Dunford , Bldg 197D, National Nuclear Data Center, Brookhaven National Laboratory, Upton, NY 11973

43. J. R. Felty, DynCorp, Advanced Technology Services, 4401 Ford Avenue, Suite 300, Alexandria, VA 22302-1432

44. S. Frankle, Los Alamos National Laboratory, XTM, MSB226, P.O. Box 1663, Los Alamos, NM 87545

45. Adolf Garcia, DOE-ID, 850 Energy Drive, MS 1154, Idaho Falls, ID 83401-1563

46. C. Lubitz, Knolls Atomic Power Laboratory, P. O. Box 1072, Schnectady, NY 12301

47. R. E. MacFarlane, Los Alamos National Laboratory, T2, MS342, Los Alamos, NM 87545

48. Prof. Aquilino Senra Martinez, Programa de Engenharia Nuclear, COPPE/UFRJ, Caixa Postal -68509, Rio de Janeiro, RJ, CEP: 21945 Brazil

49. T. McLaughlin, Los Alamos National Laboratory, P.O. Box 1663, ESH-6, Los Alamos, NM 87545

50. R. Mosteller, Los Alamos National Laboratory , TSA-10, MS K551, Los Alamos, NM 87545

51. Office of Scientific and Technical Information, U.S. Department of Energy, P.O. Box 62, Oak Ridge, TN 37831
52. Office of the ORNL Site Manager, Department of Energy, Oak Ridge National Laboratory, P.O. Box 2008, Oak Ridge, TN 37831
53. O.Ozer, Electric Power Research Institute, 3412 Hillview Ave., Palo Alto, CA 94304
54. M. Williams, Nuclear Science Center, Louisiana State University, Baton Rouge, LA 70803